1

Two Carrier Semiconductor Device Models with Geometric Structure and Symmetry Properties

Gui-Qiang Chen and Joseph W. Jerome

Northwestern University

Chi-Wang Shu

Brown University

Dehua Wang

Northwestern University

Abstract

We introduce a novel two carrier (electro) hydrodynamic model, which incorporates higher dimensional geometric effects into a one dimensional model. A rigorous mathematical analysis is carried out for the evolution system in the case of piezotropic flow, including realistic carrier coupling. The proofs are constructive in nature, making use of generalized Godunov schemes with a novel fractional step, steady-state component, and compensated compactness. Two important applications are studied. We simulate: (1) the GaAs device in the notched oscillator circuit; and, (2) a MESFET channel, and its steady-state symmetries. The first of these applications is the well known Gunn oscillator, and we are able to replicate Monte-Carlo simulations, based upon the Boltzmann equation. For the second application, we observe the effect of a symmetry breaking parameter, the potential bias on the drain.

1 Introduction

In previous work, we have studied one and two dimensional semiconductor devices over a wide range of parameters, via the hydrodynamic model. Important characteristics of this model include heat conduction, relaxation, and electrical forcing and heating terms. In particular, carrier transport occurs in a self-consistent electric field. The model is decidedly more complex than the standard gas dynamics model, and therefore permits more diverse solution behavior. In [18]–[20], n^+-n-n^+ diodes in one dimension and MESFETS in two dimensions were simulated via an essentially nonoscillatory shock capturing algorithm (ENO). In this work, we allow for the additional generalization of multi-species and geometric source terms. Such generality is driven by significant applications. For example, it has become customary among device physicists to differentiate the same particle carrier (say, electrons) on the basis of its energy valley occu-

pancy. Monte-Carlo simulations of the Boltzmann equation routinely proceed in this manner. Thus, we are able to simulate two-valley Gallium Arsenide diodes, and examine their oscillatory behavior when coupled to simple circuits. This application is called the Gunn oscillator in the device literature. Also, we are able to examine the symmetry breaking properties of the potential bias on the drain of a MESFET transistor, and compare in detail the solutions of the two dimensional model with those of the one dimensional model with spherical symmetry.

We present a comprehensive mathematical analysis for the reduced version of the multi-species model with geometric source terms, viz., the piezotropic model, with pressure a specific function of density. In the remainder of the introduction, we briefly describe the two applications, and summarize our mathematical results.

1.1   Description of the Gunn Oscillator

The equations describing an RLC tank circuit, connected to a Gunn diode, are:

$$V_D(t) = V_B - L\frac{dI(t)}{dt}, \;\; I(t) = I_d(t) + C\frac{dV_D(t)}{dt} + \frac{V_D(t)}{R}, \qquad (1.1)$$

where $V_D(t)$ is the voltage at the device terminal, V_B is the bias voltage, $I(t)$ is the current flowing through the battery, and C is the total capacitance, which includes the so-called cold capacitance. $I_d(t)$ is the particle current, which is spatially constant throughout the diode. In [22], a Monte-Carlo simulation of the Boltzmann equation was used to update $I_d(t)$. Earlier, a single valley hydrodynamic model was used in simulation by the authors of [9], whereas here we employ a two-valley hydrodynamic model. The coupling terms and the system have the structure of [1]. As derived in [17], each carrier in the diode then satisfies a system of the form:

$$\begin{cases} \partial_t\rho + \nabla\cdot(\rho v) = C_\rho, \\ \partial_t m + v(\nabla\cdot m) + (m\cdot\nabla)v = -\frac{e}{m^*}\rho F - \nabla(\rho k_b \mathcal{T}/m^*) + C_m, \\ \partial_t E + \nabla\cdot(v\,E) = -\frac{e}{m^*}\rho v\cdot F - \nabla\cdot(v\rho k_b \mathcal{T}/m^*) + \nabla\cdot(\kappa\nabla\mathcal{T}) + C_E. \end{cases} \qquad (1.2)$$

Here, ρ denotes particle mass density, related to concentration n and effective mass m^* via $\rho = m^*n$, m denotes particle momentum density, related to velocity v through $m = \rho v$, and E the mechanical energy density. F denotes the electric field, $\mathcal{T}$ the carrier temperature, e the charge modulus, κ the heat conductivity, k_b Boltzmann's constant, and C_ρ, C_m, and C_E denote relaxation expressions. The systems are coupled through the Poisson electrostatic equation as well. We shall give greater detail in §4. There, we shall interpret the two copies of (1.2) as describing GaAs electron carriers associated with lower (Γ) and middle (L) energy valleys. The occasional use of the third (upper) valley is not made here.

1.2   Basic MESFET Description

Next we describe a two dimensional MESFET of the size $0.6 \times 0.2\mu m^2$. The source and the drain each occupies $0.1\mu m$ at the upper left and the upper

right, respectively, with a gate occupying $0.2\mu m$ at the upper middle (Fig. 1). The doping is defined by $n_d = 3 \times 10^5 \mu m^{-3}$ in $[0, 0.1] \times [0.15, 0.2]$ and in $[0.5, 0.6] \times [0.15, 0.2]$, and $n_d = 1 \times 10^5 \mu m^{-3}$ elsewhere. We apply, at the drain, voltage biases varying up to $vbias = 2$V. This bias has been described earlier as a symmetry breaking parameter, and we shall investigate this in detail in the sequel. The gate is a Schottky contact, with negative voltage bias up to $vgate = -0.8$V and very low concentration value $n = 3.8503 \times 10^{-8} \mu m^{-3}$ (following Selberherr [27]). The lattice temperature is taken as $\mathcal{T}_0 = 300$ K. The mathematical model for the MESFET is the system (1.2), coupled to Poisson's electrostatic equation.
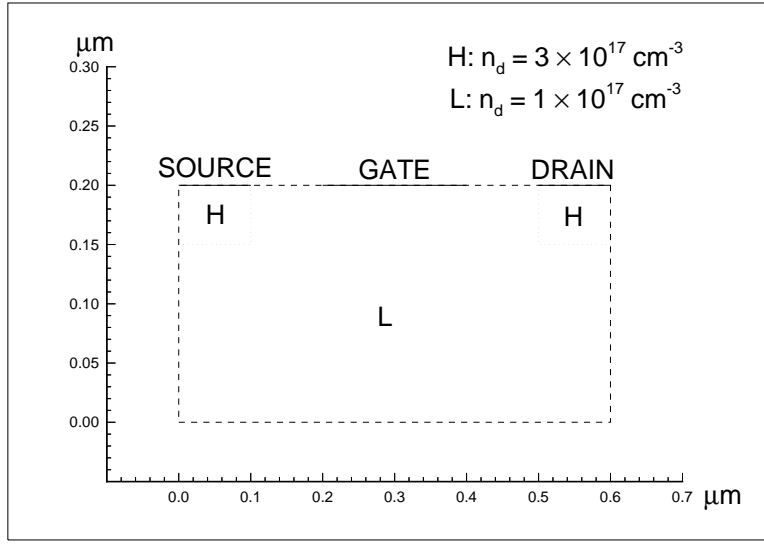
Fig. 1: Two dimensional MESFET. The geometry and the doping n_d.

1.3 Mathematical Results: A Well Posed Reduced Model

Consider a reduced model, the compressible, two carrier, Euler-Poisson equations:

$$\begin{cases} \partial_t \rho_i + \nabla \cdot \vec{m}_i = R_i(\rho_1, \rho_2), \\ \partial_t \vec{m}_i + \nabla \cdot \left(\frac{\vec{m}_i \otimes \vec{m}_i}{\rho_i} \right) + \nabla p(\rho_i) = \rho_i \nabla \phi - \frac{\vec{m}_i}{\tau_i} + \vec{H}_i(\rho_1, \rho_2, E_1, E_2), \quad (1.3) \\ \Delta \phi = \rho_1 + \rho_2 - n_d(\vec{x}), \qquad i = 1, 2, \quad \vec{x} \in \mathbf{R}^N, \end{cases}$$

where $\rho_i(\vec{x}, t)$, $\vec{m}_i(\vec{x}, t)$, and $\phi(\vec{x}, t)$ denote the density, the momentum, and the potential of the flows, respectively, and $p(\rho_i) = \rho_i^\gamma / \gamma$, $\gamma > 1$, is the pressure, $E_i = \frac{\rho_i^{\gamma-1}}{\gamma(\gamma-1)} + \frac{|\vec{m}_i|^2}{2\rho_i^2}$ is the mechanical energy, $\tau_i > 0$ is the momentum relaxation time, and $n_d(\vec{x})$ is the doping profile. For simplicity, in this mathematical model, we have selected units in which e/m_i^* has been absorbed into the units of ρ_i, $i = 1, 2$, the dielectric constant has been absorbed into the units of ϕ, and the charge modulus has been absorbed into the units of n_d. The initial-boundary

problem for the system (1.3) with geometric symmetry is ($1 < x < 2$, $t > 0$):

$$\begin{cases} \partial_t \rho_i + \partial_x m_i = a(x)m_i + R_i(\rho_1, \rho_2), \\ \partial_t m_i + \partial_x \left(\frac{m_i^2}{\rho_i} + p(\rho_i) \right) = a(x)\frac{m_i^2}{\rho_i} + \rho_i \phi_x - \frac{m_i}{\tau_i} + H_i(\rho_1, \rho_2, E_1, E_2), \\ \phi_{xx} = a(x)\phi_x + \rho_1 + \rho_2 - n_d(x), \qquad i = 1, 2, \end{cases}$$

(1.4)

$$\begin{cases} (\rho_i, m_i)|_{t=0} = (\rho_{i0}(x), m_{i0}(x)), \\ m_i|_{x=1} = m_i|_{x=2} = 0, \qquad \phi|_{x=1} = \phi_1(t) \in L^\infty, \quad \phi|_{x=2} = \phi_2(t) \in L^\infty, \end{cases}$$

(1.5)

where the field term ϕ_x is nonlocal (self-consistent) and $a(x)$ is a C^1 function that can be represented by $a(x) = -A'(x)/A(x)$. The function $A(x)$ describes the cross-sectional area at x in a variable-area duct such as a nozzle channel, and $A(x) = \frac{2\pi^{N/2}}{\Gamma(N/2)} x^{N-1}$ for spherically symmetric flow in N dimensions, such as in the MESFET, for the one carrier case we test.

The Euler-Possion equations for two carriers with $a(x) = 0$ have been studied for some special couplings: The case $R_i = H_i = 0$ in [26] by the Godunov scheme with fractional step techniques and the case $R_i = (1 - \rho_1\rho_2)Q(\rho_1, \rho_2)$, $H_i = 0$, $0 \le Q(\rho_1, \rho_2) \le \frac{Q_0}{1+\rho_1+\rho_2}$ in [14] by the viscosity method. The system for one carrier with general $a(x) \in C^1$ is solved in [8].

We develop a new shock capturing numerical scheme and apply this scheme to construct global entropy solutions to the system (1.4–1.5) with nonzero $a(x)$ and general R_i and H_i. More precisely, we consider the following coupling terms $R_i(\rho_1, \rho_2)$ and $H_i(\rho_1, \rho_2, E_1, E_2)$:

(A1) R_i and H_i are Lipschitz functions in the variables $\rho_1 \ge 0$, $\rho_2 \ge 0$, E_1, and E_2.

(A2) There exist a constant $C > 0$ and a decomposition of R_i: $R_i(\rho_1, \rho_2) = R_i^+(\rho_1, \rho_2) - R_i^-(\rho_1, \rho_2)$ with $R_i^\pm(\rho_1, \rho_2) \ge 0$ such that, for all ρ_1, $\rho_2 > 0$ and $i = 1, 2$,

$$R_i(\rho_1, \rho_2) \le C, \qquad |H_i(\rho_1, \rho_2, E_1, E_2)| \le C\rho_i;$$
$$R_i^+(\rho_1, \rho_2) \le C\rho_i, \text{ if } R_i^+(\rho_1, \rho_2) \ge R_i^-(\rho_1, \rho_2) \text{ and } \rho_i \ge c_0;$$
$$0 < R_i^-(\rho_1, \rho_2) \le C\rho_i, \text{ if } R_i^+(\rho_1, \rho_2) < R_i^-(\rho_1, \rho_2),$$

where $c_0 = (\theta/(\theta+1))^{1/\theta}$ with $\theta = (\gamma - 1)/2$.

We then have the following theorem, which is a synopsis of theorems 3.9 and 3.10 of the sequel:

Theorem 1.1 *Let $a(x)$ be a C^1 function and $1 < \gamma \le 5/3$. Let $R_i(\rho_1, \rho_2)$ and $H_i(\rho_1, \rho_2, E_1, E_2)$ satisfy Assumptions (A1)-(A2). Then there exists a sequence of approximate solutions $(\rho_i^h(x,t), m_i^h(x,t))$, for $i = 1, 2$, converging a.e. to an entropy solution $(\rho_i(x,t), m_i(x,t))$, of (1.4–1.5) such that $0 \le \rho_i(x,t) \le C(T) < \infty$, $|m_i(x,t)/\rho_i(x,t)| \le C(T) < \infty$, for $0 \le t \le T < \infty$, $x \in \mathbf{R}$, a.e.*

Assumptions (A1)–(A2) are in fact quite general. For example, $R_i = 0$, $R_i = \frac{1-\rho_1\rho_2}{1+\rho_1+\rho_2}$, $R_i = \frac{(-1)^i(\rho_1-\rho_2)}{1+\rho_1+\rho_2}$, $H_i = 0$, and $H_i = \frac{\rho_i E_i}{1+E_1+E_2}$ are in this class.

Since $a(x)$ is not equal to zero, the nonlinear resonance between characteristic modes and the geometric source terms occurs at the sonic state, that is, some of the characteristic speeds and the source speed coincide at the sonic state. Such a nonlinear resonance causes extra difficulties (cf. [5, 6], [13], [15], [23, 24], [16]). Recently, an efficient shock capturing scheme was developed in [5, 6] to solve the Euler equations with geometric structure by incorporating the steady-state solutions with the Godunov scheme. Our problem (1.4) and (1.5) involves both the geometrical source terms and nonlocal source terms.

Due to the geometric source terms, we adopt the approach of Chen-Glimm [5, 6]. One of the key ideas of this approach is to use the piecewise approximate steady-state solutions, which incorporate the geometric source terms, to replace the piecewise constants from the Riemann solutions as the building blocks. The main difficulty in achieving this is that, in the transonic case, no smooth steady-state solution exists, and an approximate steady-state solution, including a standing shock, has to be introduced, satisfying some important properties similar to those of the smooth solution in each cell: (a) The oscillation of the steady-state solution around the Godunov value must be of the same order as the cell length to obtain the L^∞ estimate for the convergence arguments; (b) The difference between the average of the steady-state solution over each cell and the Godunov value must be higher than first order in the cell length to ensure the consistency between the corresponding approximate solutions and the Euler equations. These requirements are naturally satisfied by smooth steady-state solutions that are bounded away from the sonic state in the cell. The sonic difficulty is overcome, as in experimental physics, by using the additional standing shock with continuous mass and adjusting its left state and right state in the density and its location to control the growth of the density. This construction considerably improves the traditional Godunov scheme for this case.

Due to the nonlocal source terms, we also incorporate the fractional step procedure into our construction of approximate solutions with the steady-state solutions as their fundamental building blocks. First we solve Poisson's equation to get ϕ_x, which is the nonlocal term. To obtain the uniform bound of the approximate solutions, we estimate the Riemann invariants, for which the nonlocal term is involved. For the case $a(x) = 0$, one has the conservation of particles. For the case $a(x) \neq 0$, one does not have such a conservation principle because of the geometric source terms. Therefore we have to make a proper estimate on the nonlocal term in order to get the uniform estimate of the approximate solutions. For this purpose, we use the conservation of mass in a different but equivalent way. We change the definition of the Godunov values in the scheme and prove a new property of the steady-state solution. Then we can make a new estimate on the nonlocal term, which is sufficiently robust so that the uniform estimate can be achieved. To estimate the H^{-1} compactness of the weak entropy dissipation measures, we first make the estimates on the mechanical entropy pair, which will also be used later to prove the convergence and existence. Because of the different definition of the Godunov values, we must prove the existence separately for the first and the second equations of (1.4), and use the new property of the

steady-state solution. Some extra terms from the fractional step procedure must be taken into account.

These requirements enable us to deduce the strong convergence of the approximate solutions with the aid of a compactness framework (see Chen [2, 3]). The framework takes the vacuum into account in correct physical variables (ρ, m) near the vacuum, rather than the variables (ρ, u) ($u :=$ velocity) that are physically incorrect on the vacuum. The compactness framework we use was proved in [12] for the case $\gamma = 1 + \frac{2}{2\ell+1}$, $\ell \geq 2$, and in [2, 11] (also see [3]) for the general case of gases with $1 < \gamma \leq 5/3$. Finally, the new existence theorem for the global weak solution to the initial-boundary problems of (1.3–1.4), with nonlocal source terms, is established with the aid of this framework.

2   The Mathematical Framework

Here we provide the framework for the proof of Theorem 1.1, given in the following section.

2.1   Preliminaries

In this section, we review some basic facts about the Riemann solutions for the homogeneous systems and the steady-state solutions.

Consider the homogeneous system:

$$u_t + f(u)_x = 0, \quad 1 < x < 2, \tag{2.1}$$

where $u = (\rho, m)^\top$ and $f(u) = (m, \frac{m^2}{\rho} + p(\rho))^\top$ with $p(\rho) = \rho^\gamma/\gamma$, $\gamma > 1$.

The eigenvalues are

$$\lambda_1 = \frac{m}{\rho} - \rho^\theta, \quad \lambda_2 = \frac{m}{\rho} + \rho^\theta,$$

where $\theta = \frac{\gamma-1}{2}$. The two characteristic fields are genuinely nonlinear.

The Riemann invariants are

$$w = \frac{m}{\rho} + \frac{\rho^\theta}{\theta}, \quad z = \frac{m}{\rho} - \frac{\rho^\theta}{\theta}.$$

The discontinuity in the weak solution of (2.1) satisfies the Rankine-Hugoniot condition:

$$\sigma(u - u_0) = f(u) - f(u_0), \tag{2.2}$$

where σ is the propagation speed of the discontinuity, and u_0 and u are the corresponding left state and right state, respectively. A discontinuity is a shock if it satisfies the entropy condition:

$$\sigma(\eta(u) - \eta(u_0)) - (q(u) - q(u_0)) \geq 0, \tag{2.3}$$

for any convex entropy pair (η, q). The shock with speed $\sigma = 0$ is called the standing shock.

Consider the Riemann problem consisting of (2.1) with initial data,

$$u|_{t=0} = \begin{cases} u_-, & x < x_0, \\ u_+, & x > x_0, \end{cases} \tag{2.4}$$

where $x_0 \in (1, 2)$, $u_\pm = (\rho_\pm, m_\pm)^\top$, and $\rho_\pm \geq 0$ and $m_\pm$ are constants satisfying $\left|\frac{m_\pm}{\rho_\pm}\right| < \infty$. There are two distinct types of rarefaction waves and shock waves.

For the Riemann problem with data (2.4) and the Riemann initial-boundary problem of (2.1) with data:

$$u|_{t=0} = u_+, \quad m|_{x=1} = 0, \tag{2.5}$$

we have the following facts regarding the solutions.

Lemma 2.1 *There exists a piecewise smooth entropy solution $u(x, t)$ for each problem of (2.4) and (2.5) satisfying*

$$\begin{cases} w(u(x,t)) \leq \max(w(u_-), w(u_+)), \\ w(u(x,t)) - z(u(x,t)) \geq 0, \end{cases} \tag{2.6}$$

and, for (2.4),
$$z(u(x,t)) \geq \min(z(u_-), z(u_+)),$$

and, for (2.5),
$$z(u(x,t)) \geq \min(z(u_+), 0).$$

Lemma 2.2 *For the Riemann problem (2.4), the region*

$$\sum = \{(\rho, m) : w \leq w_0, z \geq z_0, w - z \geq 0\}$$

is an invariant region of (2.1). For the Riemann initial-boundary problem (2.5), the region

$$\sum = \{(\rho, m) : w \leq w_0, z \geq z_0, w - z \geq 0\}, \quad z_0 \leq 0 \leq \frac{w_0 + z_0}{2},$$

is an invariant region of (2.1). That is, if the Riemann data lie in $\sum$, then the Riemann solutions $u(x, t) \in \sum$ and $\frac{1}{b-a}\int_a^b u(x,t)dx \in \sum$.

For the Riemann initial-boundary problem of (2.1) with data:

$$u|_{t=0} = u_-, \quad m|_{x=2} = 0, \tag{2.7}$$

we have the similar results to those for (2.5) in the above two lemmas.

A pair of mappings $(\eta, q) : \mathbf{R}^2 \rightarrow \mathbf{R}^2$ is called an entropy-entropy flux pair if $\nabla q = \nabla \eta \nabla f$. If $\tilde{\eta}(\rho, v) \equiv \eta(\rho, \rho v)$ satisfies $\tilde{\eta}(0, v) = 0$, for any fixed $v = \frac{m}{\rho}$, then η is called a weak entropy. For example, the mechanical energy-energy flux pair

$$\eta_* = \frac{1}{2}\frac{m^2}{\rho} + \frac{1}{\gamma(\gamma - 1)}\rho^\gamma, \qquad q_* = m\left(\frac{1}{2}\frac{m^2}{\rho^2} + \frac{\rho^{\gamma-1}}{\gamma - 1}\right), \tag{2.8}$$

is a strictly convex weak entropy pair of (2.1).

Lemma 2.3 *Assume $(\rho, m)^\top = (\rho, \rho v)^\top$ is a Riemann solvtion of (2.1) satisfying $0 \leq \rho \leq C'$, $|v| \leq C'$, for some constant $C' > 0$; then there exists a constant $C > 0$ such that*

$$|\nabla \eta| \leq C, \; |\nabla q| \leq C; \quad |u^\top \nabla^2 \eta u| \leq C u^\top \nabla^2 \eta_* u; \quad |\sigma[\eta] - [q]| \leq C(\sigma[\eta_*] - [q_*]),$$

for any weak entropy pair (η, q), where u is any vector and the constant C is independent of u.

Next we revisit some important properties of the steady-state solutions (see [5, 6, 8]). Consider the system of steady-state equations with boundary condition:

$$\begin{cases} f(u)_x = a(x)g(u), \\ u|_{x=x_0} = u_0, \end{cases} \tag{2.9}$$

where

$$u = (\rho, m)^\top, \quad u_0 = (\rho_0, m_0)^\top,$$

$$f(u) = (m, \frac{m^2}{\rho} + p(\rho))^\top, \quad g(u) = (m, \frac{m^2}{\rho})^\top,$$

and

$$a(x) = -\frac{A'(x)}{A(x)}, \quad \text{with} \quad A(x) \in C^2, A(x) \geq c_0 > 0.$$

Set the sound speed: $c = \rho^\theta$. Then $M = M(u(x)) = \frac{v(x)}{c(x)}$ is the Mach number, and $M_0 = M(u_0)$.

For the nonsonic case, $|M_0^2 - 1| \geq h^\beta M_0^2$, with some $\beta \in (0, \frac{1}{6})$, $h \in (0, h_0)$ for some sufficiently small $h_0 \in (0, 1)$, (2.9) has a smooth solution.

When $|M_0^2 - 1| < h^\beta M_0^2$, the steady-state equation (2.9) does not have exact smooth solutions, but has approximate solutions satisfying

$$|f(u)_x - a(x)g(u)| \leq o(1), \quad \text{as} \quad h \to 0. \tag{2.10}$$

Near the sonic case, $K_0 \sqrt{h} \leq |M_0^2 - 1| \leq h^\beta M_0^2$, with $K_0 = 2\sqrt{\frac{\|a\|_C}{\theta}}$, take

$$\begin{cases} \rho(x) = \rho_0 \left(1 + \frac{M_0^2 - 1}{2(\theta+1)} \left(1 - \sqrt{1 - \frac{4(\theta+1)a_0}{(M_0^2 - 1)^2}(x - \tilde{x})}\right)\right), \\ m(x) = m_0(1 + a_0(x - x_0)), \end{cases} \tag{2.11}$$

where $a_0 = a(x_0)$, $\tilde{x} \in (x_0 - \frac{h}{2}, x_0 + \frac{h}{2})$. Then $u = (\rho, m)^\top$ is an approximate solution in the sense of (2.10) and satisfies

$$f(u)_x - a(x)g(u) = O(h^\beta). \tag{2.12}$$

For the transonic case, $|M_0^2 - 1| < K_0 \sqrt{h}$, we introduce a standing shock at

$x = \tilde{x}$ with left state $u_- = (\rho_{0-}, m_0)$ and right state $u_+ = (\rho_{0+}, m_0)$, where

$$\rho_{0\pm} = \rho_0 \left(\frac{\theta M_0 + 1}{\theta + 1} \right)^{\frac{1}{\theta}} (1 \pm K_0 \sqrt{h}).$$

The corresponding Mach numbers are $M_{0\pm}^2 = 1 \mp 2(\theta + 1)K_0\sqrt{h} + O(h)$. Take

$$\rho_\pm(x) = \rho_{0\pm} \left(1 + \frac{M_{0\pm}^2 - 1}{2(\theta + 1)} \left(1 - \sqrt{1 - \frac{4(\theta + 1)a_0}{(M_{0\pm}^2 - 1)^2}(x - \tilde{x})} \right) \right), \qquad (2.13)$$

with $\tilde{x} \in (x_0 - \frac{2+\theta}{4(1+\theta)}h, x_0 + \frac{2+\theta}{4(1+\theta)}h)$. Then $u(x) = (\rho(x), m(x))^\top$ defined by

$$\begin{cases} \rho(x) = \begin{cases} \rho_-(x), & x \in [x_0 - \frac{h}{2}, \tilde{x}), \\ \text{standing shock}, & x = \tilde{x}, \\ \rho_+(x), & x \in (\tilde{x}, x_0 + \frac{h}{2}], \end{cases} \\ m(x) = m_0(1 + a_0(x - x_0)), \end{cases} \qquad (2.14)$$

is an approximate solution of (2.9) with $\rho_0 \geq 0$ in the sense of (2.10) satisfying (2.12). Furthermore, we have

Lemma 2.4 *There exists a smooth steady-state solution $u(x)$ of (2.9) when $|M_0^2 - 1| \geq h^\beta M_0^2$, an approximate smooth steady-state solution $u(x)$ when $K_0\sqrt{h} \leq |M_0^2 - 1| \leq h^\beta M_0^2$, and an approximate steady-state solution including a standing shock at some $\tilde{x} \in (x_0 - \frac{2+\theta}{4(1+\theta)}h, x_0 + \frac{2+\theta}{4(1+\theta)}h)$ when $|M_0^2 - 1| < K_0\sqrt{h}$, with $h \leq h_0$, in the sense of (2.10) such that, for $x \in [x_0 - \frac{h}{2}, x_0 + \frac{h}{2}]$,*

$$\begin{cases} \rho(x) \geq 0, \\ u(x) = u_0(1 + O(\sqrt{h})), \end{cases} \qquad (2.15)$$

$$\begin{cases} w(u(x)) \leq w(u_0)(1 + Ch), & \text{if } M_0 > 0, \\ z(u(x)) \geq z(u_0)(1 + Ch), & \text{if } M_0 < 0, \end{cases} \qquad (2.16)$$

$$\frac{1}{h} \int_{x_0 - \frac{h}{2}}^{x_0 + \frac{h}{2}} u(x)dx = u_0(1 + O(h^{2(1-\beta)})), \qquad (2.17)$$

and

$$\frac{1}{h} \int_{x_0 - \frac{h}{2}}^{x_0 + \frac{h}{2}} A(x)(\rho(x) - \rho_0)dx = \rho_0 O(h^{1+\beta}), \qquad (2.18)$$

where the constant C and the bounds $O(\sqrt{h})$, $O(h^{2(1-\beta)})$, and $O(h^{1+\beta})$ depend only on the bound of $A(x)$ and are independent of M_0, and $h_0 > 0$ is sufficiently small.

2.2   The Shock Capturing Scheme

Consider the following problem:

$$\begin{cases} u_t + f(u)_x = a(x)g(u) + G(u,x,t), & 1 < x < 2, \\ u|_{t=0} = u_0(x), \\ m|_{x=1} = m|_{x=2} = 0, \end{cases} \tag{2.19}$$

where $u = (\rho, m)^\top$, $f(u)$, $g(u)$, and $a(x)$ are the same as in (2.9), and $G = (G_1, G_2) \in C$.

In this section, we construct the approximate solutions $u^h = (\rho^h, m^h)^\top = (\rho^h, \rho^h v^h)^\top$ of (2.19) in the strip $0 \le t \le T$ for any fixed $T \in (0, \infty)$, where $h = \frac{1}{M} > 0$, M a large positive integer, and $\Delta t > 0$ are the space mesh length and the time mesh length, respectively, and satisfy the following Courant-Friedrichs-Levy condition:

$$\Lambda = \max(\sup_{0 \le t \le T} |\lambda_k(\rho^h, m^h)|) \le \frac{\gamma - 1}{4(\gamma + 1)} \frac{h}{\Delta t} \le 2\Lambda,$$

where λ_k, $k = 1, 2$, are the eigenvalues of (2.19).

Assume that $u^h(x, t)$ is defined for $t < n\Delta t$. Then we define $u_j^n = (\rho_j^n, m_j^n)$ as:

$$\rho_j^n = \frac{\int_{1+(j-\frac{1}{2})h}^{1+(j+\frac{1}{2})h} A(x)\rho^h(x, n\Delta t - 0)dx}{\int_{1+(j-\frac{1}{2})h}^{1+(j+\frac{1}{2})h} A(x)dx}, \quad m_j^n = \frac{1}{h} \int_{1+(j-\frac{1}{2})h}^{1+(j+\frac{1}{2})h} m^h(x, n\Delta t - 0)dx,$$

for $2 \le j \le M - 2$;   and

$$\rho_1^n = \frac{\int_1^{1+\frac{3}{2}h} A(x)\rho^h(x, n\Delta t - 0)dx}{\int_1^{1+\frac{3}{2}h} A(x)dx}, \quad m_1^n = \frac{2}{3h} \int_1^{1+\frac{3}{2}h} m^h(x, n\Delta t - 0)dx;$$

$$\rho_{M-1}^n = \frac{\int_{2-\frac{3}{2}h}^2 A(x)\rho^h(x, n\Delta t - 0)dx}{\int_{2-\frac{3}{2}h}^2 A(x)dx}, \quad m_{M-1}^n = \frac{2}{3h} \int_{2-\frac{3}{2}h}^2 m^h(x, n\Delta t - 0)dx.$$

In the strip $n\Delta t \le t < (n+1)\Delta t$, we define $u_0^h(x, t)$ as follows:
(a). For $1 + jh \le x \le 1 + (j+1)h, 1 \le j \le M - 2$, $u_0^h(x, t)$ is an approximate solution, as described below, of the generalized Riemann problem of the system,

$$u_t + f(u)_x = a(x)g(u), \tag{2.20}$$

with initial data,

$$u|_{t=n\Delta t} = \begin{cases} u_-(x), & x < 1 + (j + \frac{1}{2})h, \\ u_+(x), & x > 1 + (j + \frac{1}{2})h, \end{cases}$$

where $u_-(x)$ and $u_+(x)$ are smooth solutions or approximate solutions of the steady-state equation,

$$f(u)_x = a(x)g(u), \tag{2.21}$$

with boundary conditions: $u_-(1+jh) = u_j^n$, $u_+(1+(j+1)h) = u_{j+1}^n$ in Section 2.1;

(b). For $1 \le x \le 1+h$, $u_0^h(x,t)$ is an approximate solution of the generalized Riemann initial-boundary problem of (2.20) with data:

$$u|_{t=n\Delta t} = u_1^+(x), \quad m|_{x=1} = 0, \tag{2.22}$$

where $u_1^+(x)$ is the smooth solution or the approximate solution of the steady-state equation (2.21) with boundary condition: $u_1^+(1+h) = u_1^n$ in Section 2.1;

(c). For $2-h \le x \le 2$, $u_0^h(x,t)$ is an approximate solution of the generalized Riemann initial-boundary problem of (2.20) with data:

$$u|_{t=n\Delta t} = u_{M-1}^-(x), \quad m|_{x=2} = 0, \tag{2.23}$$

where $u_{M-1}^-(x)$ is the smooth solution or the approximate solution of the steady-state equation (2.21) with boundary condition: $u_{M-1}^-(2-h) = u_{M-1}^n$ in Section 2.1.

We solve the above problem for small time approximately to get $u_0^h(x,t)$ by perturbing about the solution R of the corresponding Riemann problem of the homogeneous system:

$$u_t + f(u)_x = 0, \tag{2.24}$$

with data

$$u|_{t=n\Delta t} = \begin{cases} u_-(1+(j+\frac{1}{2})h-0), & x < 1+(j+\frac{1}{2})h, \\ u_+(1+(j+\frac{1}{2})h+0), & x > 1+(j+\frac{1}{2})h, \end{cases}$$

for $1+jh \le x < 1+(j+1)h$, $1 \le j \le M-2$; and the Riemann initial-boundary problems of (2.24) with data (2.22), for $1 < x \le 1+h$; and with data (2.23), for $2-h \le x < 2$.

First, let

$$R_a = \begin{cases} R = (\rho, m), & \text{if } \rho(x,t) \ge 2h^\beta, \\ (2h^\beta, m), & \text{otherwise.} \end{cases}$$

Then $R_a(x,t)$ satisfies the entropy condition on its discontinuities and

$$|R_a(x,t) - R(x,t)| \begin{cases} = 0, & \text{if } \rho(x,t) \ge 2h^\beta, \\ \le Ch^\beta, & \text{otherwise.} \end{cases}$$

As in [10], we approximate the possible existing k-th rarefaction waves (u_-^r, u_+^r), $k = 1, 2$, in $R_a(x,t)$ by finite discontinuous rays $\frac{x_l}{t} = \lambda_k(u_l^r)$ separating finite constant states u_l^r, $l = 0, 1, \cdots, L_r$, with $u_0^r = u_-^r$ and $u_{L_r}^r = u_+^r$ such that
    if $k = 1$, $w(u_{l+1}^r) = w(u_l^r) + h$, $z(u_{l+1}^r) = z(u_l^r)$, $0 \le l \le L_r - 1$,
    if $k = 2$, $z(u_{l+1}^r) = z(u_l^r) + h$, $w(u_{l+1}^r) = w(u_l^r)$, $0 \le l \le L_r - 1$.
In this way, we obtain the approximate Riemann solutions consisting of finite discontinuities separating finite constant states u_l, $l = 0, 1, \cdots, L$, with $u_0 = u_-(1+(j+\frac{1}{2})h-0)$ and $u_L = u_+(1+(j+\frac{1}{2})h+0)$. Let $\hat{u}_l(x) = (\hat{\rho}_l(x), \hat{m}_l(x))$ be the exact smooth or approximate steady-state solutions such that $\hat{u}_l(1+(j+$

$\frac{1}{2})h) = u_l$.

We use the cut-off technique and denote by $u_l(x) = (\rho_l(x), \rho_l(x)v_l(x)), 0 \leq l \leq L$, the approximate steady-state solutions as follows:

$$\rho_l(x) = \max(\hat{\rho}_l(x), 2h^\beta), \quad v_l(x) = \frac{\hat{m}_l(x)}{\hat{\rho}_l(x)}, \quad 0 \leq l \leq L.$$

The approximate solution $u_0^h(x,t) = (\rho_0^h(x,t), m_0^h(x,t))$ in the rectangle $[1 + jh, 1 + (j+1)h] \times [n\Delta t, (n+1)\Delta t)$ or $[1, 1+h] \times [n\Delta t, (n+1)\Delta t)$ or $[2 - h, 2] \times [n\Delta t, (n+1)\Delta t)$ consists of the exact or approximate steady states $u_l(x)$, $l = 0, 1, \cdots, L$, separated by the discontinuities, subject to the Rankine-Hugoniot condition, with speeds

$$\frac{dx(t)}{dt} = u_l(x(t)) + (-1)^k \sqrt{\frac{\rho_{i+1}(x(t))}{\rho_i(x(t))} \frac{p(\rho_{l+1}(x(t))) - p(\rho_l(x(t)))}{\rho_{l+1}(x(t)) - \rho_l(x(t))}},$$

with $k = 1$ or $k = 2$ determined by the k-th original elementary waves from which the discontinuity originates. Then the approximate solutions $u_0^h(x,t)$ approach the approximate Riemann solutions as $n\Delta t \rightarrow t$.

We have the following estimates on the entropy as in [5].

Lemma 2.5 *There is a constant C depending only on the uniform bound of $u_0^h(x,t)$ such that, on any approximate shock wave with speed σ_l,*

$$\sigma_l(\eta_*(u_{l+1}) - \eta_*(u_l)) - (q_*(u_{l+1}) - q_*(u_l)) > 0,$$

and

$$|\sigma_l(\eta(u_{l+1}(x(t))) - \eta(u_l(x(t)))) - (q(u_{l+1}(x(t))) - q(u_l(x(t))))$$
$$-(\sigma_l(\eta_*(u_{l+1}) - \eta_*(u_l)) - (q_*(u_{l+1}) - q_*(u_l)))| \leq Ch^{\frac{3}{2}-2\beta};$$

and on the discontinuous rays, $x = x_l(t), \sigma_l = \frac{dx_l(t)}{dt}$, of the approximate rarefaction waves,

$$|\sigma_l(\eta(u_{l+1}(x(t))) - \eta(u_l(x(t)))) - (q(u_{l+1}(x(t))) - q(u_l(x(t))))| \leq Ch^{\frac{3}{2}-2\beta},$$

for any C^2 weak entropy-entropy flux pair (η, q) and the mechanical energy-energy flux (η_*, q_*).

Finally, we define the approximate solution $u^h(x,t) = (\rho^h(x,t), m^h(x,t))$ of (2.19) in the strip $n\Delta t \leq t < (n+1)\Delta t$ by the fractional step procedure:

$$u^h(x,t) = u_0^h(x,t) + G(u_0^h(x,t), x, t)(t - n\Delta t). \qquad (2.25)$$

3 Spherically Symmetric Solutions and Nozzle Solutions

Consider the spherically symmetric solutions of (1.3) in $\mathbf{R}^N$:

$$(\rho_i(\vec{x},t), \vec{m}_i(\vec{x},t), \phi(\vec{x},t)) = (\rho_i(x,t), m_i(x,t)\frac{\vec{x}}{x}, \phi(x,t)),$$

where $x = |\vec{x}|$, $m_i(x,t) = \rho_i(x,t)v_i(x,t)$. Then (1.3–1.4) becomes

$$\begin{cases} \partial_t u_i + \partial_x f(u_i) = a(x)g(u_i) + G(u_1, u_2, x, t), & 1 < x < 2,\, t > 0, \\ u_i|_{t=0} = u_{i0}(x), \\ m_i|_{x=1} = m_i|_{x=2} = 0, & i = 1, 2, \end{cases} \tag{3.1}$$

where

$$u_i = (\rho_i, m_i)^\top, \;\; f(u_i) = (m_i, \frac{m_i^2}{\rho_i} + p(\rho_i))^\top, \;\; g(u_i) = (m_i, \frac{m_i^2}{\rho_i})^\top, \;\; G = (G_1, G_2)^\top,$$

and $a(x) = -\frac{N-1}{x} = -\frac{A'(x)}{A(x)}$, $A(x) = e^{-\int^x a(y)dy} = N\omega_N x^{N-1}$, $\omega_N = \frac{2\pi^{N/2}}{N\Gamma(N/2)}$, with

$$\begin{cases} G_1 = R_i(\rho_1, \rho_2), \\ G_2 = \rho_i\phi_x - \frac{m_i}{\tau_i} + H_i(\rho_1, \rho_2, E_1, E_2), \end{cases} \tag{3.2}$$

where

$$\phi_x = x^{1-N} \left(\int_1^x (\rho_i - D(\xi))\xi^{N-1}d\xi + c(\rho_i, t) \right), \tag{3.3}$$

$$c(\rho_i, t) = \frac{1}{\int_1^2 s^{1-N}ds} \left(\phi_2(t) - \phi_1(t) - \int_1^2 s^{1-N} \int_1^s (\rho_i - D(\xi))\xi^{N-1}d\xi ds \right).$$

We construct the approximate solutions $u_i^h(x,t) = (\rho_i^h(x,t), m_i^h(x,t))$ of (3.1) as the construction for (2.19) with $u = u_i$, $G = G(u_1, u_2, x, t)$, for each $i = 1, 2$. Then (2.25) becomes

$$\begin{cases} \rho_i^h(x,t) = \rho_{i0}^h(x,t) + R_i(\rho_{10}^h(x,t), \rho_{20}^h(x,t))(t - n\Delta t), \\ m_i^h(x,t) = m_{i0}^h(x,t) + G_2(u_{10}^h(x,t), u_{20}^h(x,t), x, t)(t - n\Delta t), \end{cases} \tag{3.4}$$

for $n\Delta t \leq t < (n+1)\Delta t$. Next we make some estimates on the approximate solutions, and then prove the convergence of the approximate solutions.

For the coupling terms $R_i(\rho_1, \rho_2)$ and $H_i(\rho_1, \rho_2, E_1, E_2)$, we assume that (A1) and (A2) of Section 1.3 hold. For ease of reference, we repeat these here. Thus, we assume that R_i and H_i are Lipschitz continuous functions of the variables $\rho_1 \geq 0$, $\rho_2 \geq 0$, E_1 and E_2; and there exists a decomposition of R_i: $R_i = R_i^+ - R_i^-$, with $R_i^\pm(\rho_1, \rho_2) > 0$, and a constant $C > 0$, such that, for all ρ_1, $\rho_2 > 0$, and each $i = 1, 2$,

$$R_i(\rho_1, \rho_2) \leq C, \tag{3.5}$$

$$\frac{R_i^+(\rho_1, \rho_2)}{\rho_i} \leq C, \quad \text{if } R_i^+(\rho_1, \rho_2) \geq R_i^-(\rho_1, \rho_2) \text{ and } \rho_i \geq \left(\frac{\theta}{\theta+1} \right)^{\frac{1}{\theta}}, \tag{3.6}$$

$$\frac{R_i^-(\rho_1, \rho_2)}{\rho_i} \leq C, \quad \text{if } R_i^+(\rho_1, \rho_2) \leq R_i^-(\rho_1, \rho_2), \tag{3.7}$$

$$\frac{|H_i(\rho_1, \rho_2, E_1, E_2)|}{\rho_i} \leq C. \tag{3.8}$$

The above assumptions are quite general as noted in the introduction.

3.1   Uniform Estimates

In this section, we shall derive the L^∞ estimates of the approximate solution $u_i^h(x,t) = (\rho_i^h(x,t), m_i^h(x,t))$ for each $i = 1, 2$. For simplicity of notation, we will drop the index i of the approximate solution $u_i^h = (\rho_i^h, m_i^h)$ and $u_{i0}^h = (\rho_{i0}^h, m_{i0}^h)$ in the proofs and denote by $C > 0$, a universal constant depending only on T, throughout this paper.

First we have the following lemma about the conservation of particles:

Lemma 3.1   *If (3.5) holds, then there exists a constant $C > 0$, which depends only on the bounds of $A(x)$ and $\rho_{i0} + \left| \frac{m_{i0}}{\rho_{i0}} \right|$, such that, for any $t \in [0, T]$ and each $i = 1, 2$,*

$$\int_1^2 \rho_{i0}^h(x,t)dx \leq C + C \max_j \{\rho_{ij}^n\} h^\beta,$$

for some n with $t \in [n\Delta t, (n+1)\Delta t)$.

Proof.   By the construction of the approximate solutions, one has

$$\int_1^2 A(x)\rho_0^h(x, (n+1)\Delta t - 0)dx + \int_{n\Delta t}^{(n+1)\Delta t} A(x(t)) \sum (\sigma[\rho_0^h] - [m_0^h])dt$$

$$= \int_1^2 A(x)\rho_0^h(x, n\Delta t + 0)dx + O(h^\beta \Delta t).$$

Using the Rankine-Hugoniot condition, one has

$$\int_{n\Delta t}^{(n+1)\Delta t} A(x(t)) \sum (\sigma[\rho_0^h] - [m_0^h])dt = 0.$$

Then

$$\int_1^2 A(x)\rho_0^h(x, (n+1)\Delta t - 0)dx$$

$$= \int_1^2 A(x)(\rho_0^h(x, n\Delta t + 0) - \rho_0^h(x, n\Delta t - 0))dx$$

$$+ \int_1^2 A(x)\rho_0^h(x, n\Delta t - 0)dx + O(h^{\beta+1}).$$

By the construction and Lemma 2.4, one has

$$\frac{1}{h} \int_{1+(j-\frac{1}{2}h)}^{1+(j+\frac{1}{2}h)} A(x)(\rho^h(x, n\Delta t - 0) - \rho_j^n)dx = 0, \tag{3.9}$$

$$\frac{1}{h} \int_{1+(j-\frac{1}{2}h)}^{1+(j+\frac{1}{2}h)} A(x)(\rho_0^h(x, n\Delta t + 0) - \rho_j^n)dx = \rho_j^n O(h^{1+\beta}). \tag{3.10}$$

Then by (3.9–3.10), and (3.5):

$$\int_1^2 A(x)(\rho_0^h(x, n\Delta t + 0) - \rho_0^h(x, n\Delta t - 0))dx$$

$$= \sum_j \int_{1+(j-\frac{1}{2})h}^{1+(j+\frac{1}{2})h} A(x)(\rho_0^h(x, n\Delta t + 0) - \rho_j^n)dx$$

$$+ \sum_j \int_{1+(j-\frac{1}{2})h}^{1+(j+\frac{1}{2})h} A(x)(\rho_j^n - \rho_0^h(x, n\Delta t - 0))dx$$

$$= \sum_j \int_{1+(j-\frac{1}{2})h}^{1+(j+\frac{1}{2})h} A(x)R_i(\rho_{10}^h(x, n\Delta t - 0), \rho_{20}^h(x, n\Delta t - 0))\Delta t dx$$

$$+ \sum_j \rho_j^n O(h^{2+\beta})$$

$$\leq \sum_j \rho_j^n O(h^{2+\beta}) + Ch,$$

and

$$\int_1^2 A(x)\rho_0^h(x, (n+1)\Delta t - 0)dx$$

$$\leq \int_1^2 A(x)\rho_0^h(x, n\Delta t - 0)dx + \sum_j \rho_j^n O(h^{2+\beta}) + O(h^{1+\beta}) + Ch.$$

Therefore, by induction on n, we have, for any positive integer n,

$$\int_1^2 A(x)\rho_0^h(x, n\Delta t - 0)dx \leq \int_1^2 A(x)\rho_0^h(x, 0)dx + \sum_j \rho_j^n O(h^{1+\beta}) + O(h^\beta) + C.$$

For any $t \in [0, T]$, $t \in [n\Delta t, (n+1)\Delta t)$ for some n, then, by the construction of the approximate solutions and the Rankine-Hugoniot condition, one has

$$\int_1^2 A(x)\rho_0^h(x, t)dx = \int_1^2 A(x)\rho_0^h(x, n\Delta t + 0)dx + O(h^\beta \Delta t)$$

$$\leq \int_1^2 A(x)\rho_0(x)dx + \sum_j \rho_j^n O(h^{1+\beta}) + O(h^\beta) + C.$$

Since $A(x) \geq N\omega_N$ for any $x \in (1, 2)$, Lemma 3.1 follows.

$\square$

Let $\Pi_T = [1, 2] \times [0, T]$. We have the following uniform estimate.

Theorem 3.2 *Suppose that (3.5–3.8) hold and there exists a constant $C > 0$ such that $0 < \rho_{i0}(x) \leq C$, and $|v_{i0}(x)| \leq C$ for all $x \in (1, 2)$, $i = 1, 2$. Then, for $h \leq h_0$, there exists a positive constant $C(T)$, independent of h and τ_i, such*

that, for each $i = 1, 2$,

$$h^\beta \leq \rho_i^h(x,t) \leq C(T), \quad |v_i^h(x,t)| \leq C(T), \quad (x,t) \in \Pi_T.$$

Proof.   Suppose, for small h and each $i = 1, 2$,

$$\sup_{(x,t)} \rho_i^h(x,t) \leq \frac{1}{h^\beta}, \quad \text{and} \quad \sup_{(x,t)} |v_{i0}^h(x,t)| \leq \frac{1}{h^\beta},$$

and there exists $K(h)$ satisfying $K(h) \to \infty$ as $h \to 0$ such that

$$\sup_{(x,t)} \rho_{i0}^h(x,t) \leq K(h), \quad i = 1, 2,$$

and then

$$\sup_{(x,t)} |R_i(\rho_{10}^h(x,t), \rho_{20}^h(x,t))| \leq \frac{1}{h^\beta}.$$

Thus, Lemma 3.1 implies

$$\int_1^2 \rho_0^h(x,t)dx \leq C, \quad \forall\, t \in [0,T].$$

By the construction of (ρ^h, m^h), we have $\rho_0^h(x,t) \geq 2h^\beta$, for $(x,t) \in \Pi_T$. Then for $t \in [n\Delta t, (n+1)\Delta t)$, by (3.4),

$$\rho^h(x,t) \geq 2h^\beta - \frac{Ch}{h^\beta} \geq h^\beta.$$

By (3.3), one has

$$|\phi_x| \leq C.$$

In $n\Delta t \leq t < (n+1)\Delta t$, we estimate the Riemann invariant w using (3.4) and (3.1). Note that

$$\left| \frac{R_i}{\rho_0^h}(t - n\Delta t) \right| \leq \frac{1}{h^\beta} \cdot \frac{Ch}{2h^\beta} \leq Ch^{1-2\beta}.$$

Then, by (3.1) and (3.8), we have the following estimates:

$$w(v^h(x,t))$$
$$= \left(\frac{m_0^h}{\rho_0^h} + \left(\phi_x - \frac{m_0^h}{\tau_i \rho_0^h} + \frac{H_i}{\rho_0^h} \right)(t - n\Delta t) \right) \left(1 + \frac{R_i}{\rho_0^h}(t - n\Delta t) \right)^{-1}$$
$$+ \frac{(\rho_0^h)^\theta}{\theta} \left(1 + \frac{R_i}{\rho_0^h}(t - n\Delta t) \right)^\theta$$
$$= \left(\frac{m_0^h}{\rho_0^h} + \left(\phi_x - \frac{m_0^h}{\tau_i \rho_0^h} + \frac{H_i}{\rho_0^h} \right)(t - n\Delta t) \right) \left(1 - \frac{R_i}{\rho_0^h}(t - n\Delta t) + O(h^{2-4\beta}) \right)$$
$$+ \frac{(\rho_0^h)^\theta}{\theta} \left(1 + \theta \frac{R_i}{\rho_0^h}(t - n\Delta t) + O(h^{2-4\beta}) \right)$$

$$\leq \left(w(v_0^h(x,t)) + \left(\phi_x + \frac{H_i}{\rho_0^h} - \frac{m_0^h}{\tau_i \rho_0^h} \right)(t - n\Delta t) \right)(1 + O(\Delta t)) + C\Delta t$$

$$+ \left(\phi_x + \frac{H_i}{\rho_0^h} - \frac{m_0^h}{\tau_i \rho_0^h} \right)(t - n\Delta t) \left(-\frac{R_i}{\rho_0^h}(t - n\Delta t) \right)$$

$$- (u_0^h - (\rho_0^h)^\theta) \frac{R_i}{\rho_0^h}(t - n\Delta t)$$

$$\leq \left(w(u_0^h(x,t)) \left(1 - \frac{t - n\Delta t}{2\tau_i} \right) - z(u_0^h(x,t)) \frac{t - n\Delta t}{2\tau_i} \right)(1 + O(\Delta t))$$

$$+ C\Delta t + (t - n\Delta t) I_1,$$

where

$$I_1 = -(v_0^h - (\rho_0^h)^\theta) \frac{R_i}{\rho_0^h}.$$

Similarly,

$$z(u^h(x,t)) \geq \left(z(u_0^h(x,t)) \left(1 - \frac{t - n\Delta t}{2\tau_i} \right) - w(u_0^h(x,t)) \frac{t - n\Delta t}{2\tau_i} \right)(1 + O(\Delta t))$$

$$- C\Delta t + (t - n\Delta t) I_2,$$

where

$$I_2 = -(v_0^h + (\rho_0^h)^\theta) \frac{R_i}{\rho_0^h}.$$

It suffices to consider the cases $w(u_0^h(x,t)) \geq 1$ and $z(u_0^h(x,t)) \leq -1$. When $w(v_0^h(x,t)) \geq 1$,

$$v_0^h \geq 1 - \frac{(\rho_0^h)^\theta}{\theta}.$$

If $R_i \geq 0$, then

$$I_1 \leq - \left(1 - \frac{\theta + 1}{\theta}(\rho_0^h)^\theta \right) \frac{R_i}{\rho_0^h},$$

in the case $(\rho_0^h)^\theta \leq \frac{\theta}{\theta+1}$, $I_1 \leq 0$; in the case $(\rho_0^h)^\theta \geq \frac{\theta}{\theta+1}$, by (3.6),

$$I_1 \leq \frac{\theta + 1}{\theta}(\rho_0^h)^\theta \frac{R_i^+}{\rho_0^h} \leq C(\rho_0^h)^\theta \leq C(w(u_0^h) - z(u_0^h)).$$

If $R_i \leq 0$, then

$$I_1 = -(v_0^h - (\rho_0^h)^\theta) \frac{R_i}{\rho_0^h},$$

in the case $v_0^h \leq (\rho_0^h)^\theta$, $I_1 \leq 0$; in the case $v_0^h \geq (\rho_0^h)^\theta$, by (3.7),

$$I_1 \leq (v_0^h - (\rho_0^h)^\theta) \frac{R_i^-}{\rho_0^h} \leq C v_0^h \leq C w(u_0^h).$$

Similarly, when $z(u_0^h(x,t)) \leq -1$, $I_2 \geq 0$, or $I_2 \geq -C(z(u_0^h) - w(u_0^h))$, or $I_2 \geq$

$Cz(u_0^h)$.

By Lemma 2.4 and the construction of (ρ^h, m^h), we have

$$\begin{cases} w(u_0^h(x,t)) & \leq & \max(\sup_x w(u_0^h(x, n\Delta t + 0)), 1)(1 + C\Delta t), \\ z(u_0^h(x,t)) & \geq & \min(\inf_x z(u_0^h(x, n\Delta t + 0)), -1)(1 + C\Delta t), \end{cases}$$

for $h \leq h_0$. Then

$$\begin{aligned} w(u^h(x,t)) & \leq & \max(\sup_x w(u_0^h(x, n\Delta t + 0)), 1)(1 + C\Delta t)\left(1 - \frac{t - n\Delta t}{2\tau}\right) \\ & & - \min(\inf_x z(u_0^h(x, n\Delta t + 0)), -1)(1 + C\Delta t)\frac{t - n\Delta t}{2\tau} + C\Delta t. \end{aligned}$$

Similarly, we have

$$\begin{aligned} z(u^h(x,t)) & \geq & \min(\inf_x z(u_0^h(x, n\Delta t + 0)), -1)(1 + C\Delta t)\left(1 - \frac{t - n\Delta t}{2\tau}\right) \\ & & - \max(\sup_x w(u_0^h(x, n\Delta t + 0)), 1)(1 + C\Delta t)\frac{t - n\Delta t}{2\tau} + C\Delta t. \end{aligned}$$

Note that

$$\begin{cases} w(u_j^n) = w(\bar{u}_j^n)(1 + O(h)), \\ z(u_j^n) = z(\bar{u}_j^n)(1 + O(h)), \end{cases}$$

with $\bar{u}_j^n = \frac{1}{h} \int_{1+(j-\frac{1}{2})h}^{1+(j+\frac{1}{2})h} u^h(x, n\Delta t - 0)dx$.

Set $M_n = \max(\sup_x w(u_0^h(x, n\Delta t + 0)), -\inf_x z(u_0^h(x, n\Delta t + 0)), 1)$. Then

$$M_{n+1} \leq M_n(1 + C\Delta t) + C\Delta t.$$

Thus,

$$\begin{aligned} M_{n+1} & \leq M_0(1 + C\Delta t)^{n+1} + C(n+1)\Delta t(1 + C\Delta t)^n \\ & \leq M_0(1 + C\Delta t)^{\frac{T}{\Delta t}+1} + CT(1 + C\Delta t)^{\frac{T}{\Delta t}} \leq C(T). \end{aligned}$$

This means:

$$\begin{cases} w(u^h(x,t)) \leq C(T)(1 + C\Delta t) + K\Delta t \leq C(T), \\ -z(u^h(x,t)) \leq C(T)(1 + C\Delta t) + K\Delta t \leq C(T), \\ w(u^h(x,t)) - z(u^h(x,t)) \geq \frac{2h^{\beta\theta}}{\theta}. \end{cases}$$

Therefore, there exists a constant $C(T) > 0$ such that

$$h^\beta \leq \rho^h(x,t) \leq C(T), \quad |v^h(x,t)| = \left|\frac{m^h(x,t)}{\rho^h(x,t)}\right| \leq C(T),$$

where the constant $C(T)$ is independent of h and τ.

Choose $h_0 > 0$ such that, for $h \leq h_0$, $C(T) < \min(\frac{1}{h^\beta}, K(h))$, then

$$h^\beta \leq \rho^h(x,t) \leq C(T) < \frac{1}{h^\beta}, \quad |v^h(x,t)| \leq C(T) < K(h).$$

This completes the proof.

$\square$

3.2 H^{-1} Compactness of Entropy Measures

We need the following basic lemma (cf. [3, 11, 29]) to prove the H^{-1} compactness of entropy measures for the approximate solutions (ρ_i^h, m_i^h).

Lemma 3.3 *Let $\Omega \subset \mathbf{R}^N$ be a bounded domain. Then*

$$(\text{compact set of } W^{-1,q}(\Omega)) \cap (\text{bounded set of } W^{-1,r}(\Omega))$$

$$\subset (\text{compact set of } W^{-1,2}_{\text{loc}}(\Omega)),$$

where q and r are constants, $1 < q \le 2 < r < \infty$.

Theorem 3.4 *If (3.5–3.8) hold, and $\{u_i^h\}$, $i = 1, 2$, are the approximate solutions, then the measure sequence,*

$$\eta(u_i^h)_t + q(u_i^h)_x$$

is a compact subset of $H^{-1}_{\text{loc}}(\Omega)$ for all weak entropy pairs (η, q), where Ω is any bounded and open set in Π_T.

Proof. We drop the index i of u_i^h and u_{i0}^h in the proof. For any test function $\psi \in C_0^1(\Pi_T)$, we have

$$\int\int_{\Pi_T} (\eta(u^h)\psi_t + q(u^h)\psi_x)dxdt = A(\psi) + M(\psi) + N(\psi) + L(\psi) + \Sigma(\psi) + E(\psi). \tag{3.11}$$

Here,

$$A(\psi) = \int\int_{\Pi_T} \left((\eta(u^h) - \eta(u_0^h))\psi_t + (q(u^h) - q(u_0^h))\psi_x\right) dxdt,$$

$$M(\psi) = \int_1^2 \psi(x, T)\eta(u_0^h(x, T))dx - \int_1^2 \psi(x, 0)\eta(u_0^h(x, 0))dx,$$

$$N(\psi) = -\int\int_{\Pi_T} a(x)g(u_0^h)\nabla\eta(u_0^h)\psi(x, t)dxdt,$$

$$\Sigma(\psi) = \int_0^T \sum (\sigma[\eta] - [q]) \psi(x(t), t)dt,$$

$$L(\psi) = \sum_{j,n} \int_{1+(j-\frac{1}{2})h}^{1+(j+\frac{1}{2})h} \left(\eta(u_{0-}^n) - \eta(u_{0+}^n)\right) \psi(x, n\Delta t)dx \equiv L_1(\psi) + L_2(\psi),$$

$$L_1(\psi) = \sum_{j,n} \psi_j^n \int_{1+(j-\frac{1}{2})h}^{1+(j+\frac{1}{2})h} (\eta(u_{0-}^n) - \eta(u_{0+}^n))dx,$$

$$L_2(\psi) = \sum_{j,n} \int_{1+(j-\frac{1}{2})h}^{1+(j+\frac{1}{2})h} (\eta(u_{0-}^n) - \eta(u_{0+}^n))(\psi - \psi_j^n)dx,$$

and

$$|E(\psi)| \le Ch^{\beta}\|\psi\|_{H^1},$$

where $u_{0\pm}^{n} = u_0^h(x, n\Delta t \pm 0)$, $\psi_j^n = \psi(1 + jh, n\Delta t)$, the summation in $\Sigma(\psi)$ is taken over all discontinuities in u_0^h at a fixed time t, σ is the propagating speed of the discontinuity, and $E(\psi)$ is the error term including the error in the steady-state solutions and the error near the vacuum in the construction of approximate solutions, and

$$[\eta] = \eta(u_0^h(x(t) + 0, t)) - \eta(u_0^h(x(t) - 0, t)),$$

$$[q] = q(u_0^h(x(t) + 0, t)) - q(u_0^h(x(t) - 0, t)),$$

are the jumps of $\eta(u_0^h(x, t))$ and $q(u_0^h(x, t))$ across a discontinuity $S = (x(t), t)$ in $u_0^h(x, t)$.

We shall make use of the following two lemmas:

Lemma 3.5 *For any n and $h \le h_0$,*

$$\frac{1}{h}\int_{1+(j-\frac{1}{2})h}^{1+(j+\frac{1}{2})h}(\rho^h(x, n\Delta t - 0) - \rho_j^n)dx = O(h).$$

This follows immediately from (3.9).

Lemma 3.6 *There exists a constant $C > 0$ such that*

(1). $\displaystyle\sum_{j,n}\int_{1+(j-\frac{1}{2})h}^{1+(j+\frac{1}{2})h}\int_0^1 \Theta_{\pm}^n(\eta_*, s)dsdx \le C$, *where*

$$\Theta_{\pm}^n(\eta, s) = (1 - s)(u_{0\pm}^n - u_j^n)^{\top}\nabla^2\eta(u_j^n + s(u_{0\pm}^n - u_j^n))(u_{0\pm}^n - u_j^n).$$

(2). $\displaystyle\sum_{j,n}\int_{1+(j-\frac{1}{2})h}^{1+(j+\frac{1}{2})h}|u_{0\pm}^n - u_j^n|^2dx \le C$.

This lemma follows from a similar argument in [8].

We now use these lemmas to prove Theorem 3.4.

(a). From the lemmas in Section 2.1, Section 2.2, Lemma 3.5, and Lemma 3.6,

$$|M(\psi)| \le \|\psi\|_{C_0(\Omega)}\int_1^2 \left(|\eta(u_0^h(x, T))| + |\eta(u_0^h(x, 0))|\right)dx \le C\|\psi\|_{C_0(\Omega)},$$

$$|N(\psi)| \le \|\psi\|_{C_0(\Omega)}\|\nabla\eta\|_{\infty}\|a(x)g(u_0^h)\|_{\infty}T \le C\|\psi\|_{C_0(\Omega)},$$

$$|\Sigma(\psi)| \le \|\psi\|_{C_0(\Omega)}\int_0^T\left(\sum(\sigma[\eta_*] - [q_*]) + h^{2(1-\beta)}\right)dx \le C\|\psi\|_{C_0(\Omega)},$$

and

$$|L_1(\psi)| \le \left|\sum_{j,n}\psi_j^n\int_{1+(j-\frac{1}{2})h}^{1+(j+\frac{1}{2})h}(\eta(u_{0-}^n) - \eta(u_j^n))dx\right|$$

$$+\left|\sum_{j,n}\psi_j^n\int_{1+(j-\frac{1}{2})h}^{1+(j+\frac{1}{2})h}(\eta(u_{0+}^n)-\eta(u_j^n))dx\right|$$

$$\leq \quad C\|\psi\|_{C_0}\sum_{j,n}\int_{1+(j-\frac{1}{2})h}^{1+(j+\frac{1}{2})h}\int_0^1\Theta_-^n(\eta_*,s)dsdx$$

$$+C\|\psi\|_{C_0}\sum_{j,n}\int_{1+(j-\frac{1}{2})h}^{1+(j+\frac{1}{2})h}\int_0^1\Theta_+^n(\eta_*,s)dsdx$$

$$+\|\psi\|_{C_0}(O(1)+O(h^{1-2\beta}))$$

$$\leq \quad C\|\psi\|_{C_0}.$$

Hence

$$|(M+N+L_1+\Sigma)(\psi)|\leq C\|\psi\|_{C_0},$$

that is

$$\|M+N+L_1+\Sigma\|_{C_0^*}\leq C.$$

By the embedding theorem, $(C_0(\Omega))^*\hookrightarrow W^{-1,q_1}$, for $1<q_1<2$,

$$M+N+L_1+\Sigma \quad \text{is compact in} \quad W^{-1,q_1}(\Omega).$$

(b). For any $\psi\in C_0^\alpha(\Omega)$, $\frac{1}{2}<\alpha<1$, using Hölder's inequality, we have

$$|L_2(\psi)|$$

$$\leq\sum_{j,n}\int_{1+(j-\frac{1}{2})h}^{1+(j+\frac{1}{2})h}|\psi-\psi_j^n|\left(|\eta(u_{0-}^n)-\eta(u_j^n)|+|\eta(u_{0+}^n)-\eta(u_j^n)|\right)dx$$

$$\leq C\|\psi\|_{C_0^\alpha}h^{\alpha-\frac{1}{2}}\|\nabla\eta\|_\infty$$

$$\times\left(\sum_{j,n}\int_{1+(j-\frac{1}{2})h}^{1+(j+\frac{1}{2})h}|u_{0-}^n-u_j^n|^2dx+\sum_{j,n}\int_{1+(j-\frac{1}{2})h}^{1+(j+\frac{1}{2})h}|u_{0+}^n-u_j^n|^2dx\right)^{\frac{1}{2}}$$

$$\leq Ch^{\alpha-\frac{1}{2}}\|\psi\|_{C_0^\alpha}.$$

By the Sobolev theorem: $W_0^{1,p}(\Omega)\subset C_0^\alpha(\Omega)$, $0<\alpha<1-\frac{2}{p}$, we have

$$|L_2(\psi)|\leq Ch^{\alpha-\frac{1}{2}}\|\psi\|_{W_0^{1,p}(\Omega)},\quad p>\frac{2}{1-\alpha},$$

that is

$$\|L_2\|_{W^{-1,q_2(\Omega)}}\leq Ch^{\alpha-\frac{1}{2}}\to 0,\quad h\to 0,$$

for $1<q_2<\frac{2}{1+\alpha}$.

Therefore, L_2 is compact in W^{-1,q_2}. Then,

$$M+N+L+\Sigma \quad \text{is compact in } W^{-1,q_0},$$

where $1 < q_0 = \min(q_1, q_2) < \frac{2}{1+\alpha}$.

The uniform boundedness of the approximate solutions implies

$$M + N + L + \Sigma \quad \text{is bounded in } W^{-1,r}, r > 1.$$

By Lemma 3.3, $M + N + L + \Sigma$ is compact in $\quad H_{\text{loc}}^{-1}$.

(c). Finally, for $A(\psi)$ we have

$$\|A(\psi)\| \le \int\int_{\Pi_T} (\|\nabla\eta\|_\infty + \|\nabla q\|_\infty)(|\psi_t| + |\psi_x|)|u^h - u_0^h| dx dt \le Ch\|\psi\|_{H_0^1(\Omega)}.$$

Since $C_0^\infty(\Omega)$ is dense in $H_0^1(\Omega)$, then

$$\|A\|_{H_{\text{loc}}^{-1}(\Omega)} \le Ch \to 0, \quad \text{as} \quad h \to 0,$$

so A is compact in $H_{\text{loc}}^{-1}(\Omega)$.

By $\|E\|_{H^{-1}} \le Ch^\beta \to 0$, as $h \to 0$, we know that E is compact in $H_{\text{loc}}^{-1}(\Omega)$. Therefore $A + M + N + L + \Sigma + E$ is compact in $H_{\text{loc}}^{-1}(\Omega)$, which means that $\eta(u^h)_t + q(u^h)_x$ is compact in $H_{\text{loc}}^{-1}(\Omega)$.

$\square$

3.3   Convergence and Existence

In this section, we prove that (3.1) has a weak entropy solution, which is the limit function of the approximate solutions.

Definition 3.7   *The measurable functions $u_i(x,t) = (\rho_i(x,t), m_i(x,t))$, $i = 1, 2$, are weak entropy solutions of (4.1) if, for any test function $\psi \in C_0^1(\Pi_T)$ with $\psi(1,t) = \psi(2,t) = \psi(x,T) = 0$ and, for each $i = 1, 2$,*

$$\int\int_{\Pi_T} (u_i\psi_t + f(u_i)\psi_x + (a(x)g(u_i) + G(u_1, u_2, x, t))\psi)\,dxdt$$
$$+ \int_0^T v_{i0}(x)\psi(x,0)dx = 0, \tag{3.12}$$

and, along any shock discontinuity with left state u_{i-}, right state u_{i+}, and speed σ_i,

$$\sigma_i(\eta(u_{i+}) - \eta(u_{i-})) - (q(u_{i+}) - q(u_{i-})) \ge 0, \tag{3.13}$$

for any convex weak entropy pair (η, q).

Now we introduce the following compensated compactness framework (see [2, 3]):

Lemma 3.8   *Assume that the approximate solutions $u^h = (\rho^h, m^h)$ satisfy*

(1). There is a constant $C > 0$ such that $0 \le \rho^h(x,t) \le C$, $\left|\frac{m^h(x,t)}{\rho^h(x,t)}\right| \le C$;

(2). The measure $\eta(u^h)_t + q(u^h)_x$ is compact in $H_{\text{loc}}^{-1}(\Omega)$, for all weak entropy pairs (η, q), where $\Omega \subset \Pi_T$ is any bounded and open set.

Then, for $1 < \gamma \leq 5/3$, there exists a convergent subsequence (still labeled) u^h such that $u^h(x,t) \longrightarrow u(x,t) = (\rho(x,t), m(x,t))$, a.e.

In Sections 3.1 and 3.2, we have proved that the approximate solutions $u_i^h(x,t)$, constructed in Section 3 for (3.1), satisfy (1) and (2) of Lemma 3.8. Thus, we have the following theorem:

Theorem 3.9 *Suppose (3.5–3.8) hold. Then there is a convergent subsequence (still labeled u_i^h) of the approximate solutions $u_i^h(x,t) = (\rho_i^h(x,t), m_i^h(x,t))$, $i = 1, 2$, such that*

$$u_i^h(x,t) \longrightarrow u_i(x,t) = (\rho_i(x,t), m_i(x,t)), \text{a.e.} \quad \text{as} \quad h \to 0,$$

and the function $u_i(x,t)$ is a weak entropy solution of (3.1) in the sense of Definition 3.7 and satisfies

$$0 \leq \rho_i(x,t) \leq C(T), \qquad \left| \frac{m_i(x,t)}{\rho_i(x,t)} \right| \leq C(T),$$

for $(x,t) \in \Pi_T$, where $C(T) > 0$ is a constant.

Proof. Again we drop the index i of u_i^h and u_{i0}^h in the proof. We now prove that $u(x,t)$ satisfies (3.12) and (3.13). Let $\psi \in C_0^1(\Pi_T)$ be any test function with $\psi(1,t) = \psi(2,t) = \psi(x,T) = 0$. Set $\bar{\psi}(x,t) = \frac{\psi(x,t)}{A(x)} \in C_0^1(\Pi_T)$. Then

$$\int\int_{\Pi_T} (\rho^h \psi_t + m^h \psi_x + (a(x)m^h + R_i(\rho_1^h, \rho_2^h))\psi)dxdt + \int_1^2 \rho_0^h(x)\psi(x,0)dx$$

$$= \int\int_{\Pi_T} (A(x)\rho^h \bar{\psi}_t + A(x)m^h \bar{\psi}_x + A(x)R_i(\rho_1^h, \rho_2^h)\bar{\psi})dxdt$$

$$+ \int_1^2 A(x)\rho_0^h(x)\bar{\psi}(x,0)dx$$

$$= \int\int_{\Pi_T} A(x)((\rho^h - \rho_0^h)\bar{\psi}_t + (m^h - m_0^h)\bar{\psi}_x)dxdt$$

$$+ \int\int_{\Pi_T} A(x)(R_i(\rho_1^h, \rho_2^h) - R_i(\rho_{10}^h, \rho_{20}^h))\bar{\psi}dxdt$$

$$+ \int_0^T \sum A(x(t))(\sigma[\rho_0^h] - [m_0^h])\bar{\psi}(x(t),t)dt + I_{11} + I_{12} + O(h^\beta)\|\bar{\psi}\|_{H^1},$$

where

$$I_{11} = \sum_{j,n} \bar{\psi}_j^n \int_{1+(j-\frac{1}{2})h}^{1+(j+\frac{1}{2})h} A(x)(\rho_0^h(x, n\Delta t - 0) - \rho_0^h(x, n\Delta t + 0))dx$$

$$+ \int\int_{\Pi_T} A(x)R_i(\rho_{10}^h, \rho_{20}^h)\bar{\psi}dxdt,$$

$$I_{12} = \sum_{j,n} \int_{1+(j-\frac{1}{2})h}^{1+(j+\frac{1}{2})h} A(x)(\bar{\psi} - \bar{\psi}_j^n)(\rho_0^h(x, n\Delta t - 0) - \rho_0^h(x, n\Delta t + 0))dx.$$

By the fractional step procedure and the Rankine-Hugoniot condition, one has

$$\left| \int\int_{\Pi_T} A(x)((\rho^h - \rho_0^h)\bar\psi_t + (m^h - m_0^h)\bar\psi_x)dxdt \right| \le O(h)\|\bar\psi\|_{C_0^1},$$

$$\left| \int\int_{\Pi_T} A(x)(R_i(\rho_1^h, \rho_2^h) - R_i(\rho_{10}^h, \rho_{20}^h))\bar\psi dxdt \right| \le O(h)\|\bar\psi\|_{C_0^1},$$

$$\int_0^T \sum A(x(t))(\sigma[\rho_0^h] - [m_0^h])\bar\psi(x(t), t)dt = 0.$$

¿From Proposition 3 in [25] or Lemma 2.4 in [4], and our Lemma 3.6, we have

$$\sum_{j,n} \int_{(n-1)\Delta t}^{n\Delta t} \int_{1+(j-\frac{1}{2})h}^{1+(j+\frac{1}{2})h} \left| \rho_{i0}^h(x, t) - \rho_{i0}^h(x, n\Delta t - 0) \right| dxdt \le C(T)h, \quad i = 1, 2,$$

for some constant $C(T)$. Then by the construction of $u^h(x, t)$ and Lemma 2.4, one has

$$|I_{11}|$$

$$= \left| \sum_{j,n} \bar\psi_j^n \int_{1+(j-\frac{1}{2})h}^{1+(j+\frac{1}{2})h} (A(x)(\rho^h(x, n\Delta t - 0) - \rho_j^n) \right.$$

$$\left. + A(x)(\rho_j^n - \rho_0^h(x, n\Delta t + 0)))dx \right|$$

$$+ \left| \sum_{j,n} \int_{(n-1)\Delta t}^{n\Delta t} \int_{1+(j-\frac{1}{2})h}^{1+(j+\frac{1}{2})h} A(x)(R_i(\rho_{10}^h(x, t), \rho_{20}^h(x, t))\bar\psi(x, t) \right.$$

$$\left. - R_i(\rho_{10}^h(x, n\Delta t - 0), \rho_{20}^h(x, n\Delta t - 0))\bar\psi_j^n)dxdt \right|$$

$$\le \|\psi\|_{C_0^1} O(h^\beta) + \sum_{j,n} \int_{(n-1)\Delta t}^{n\Delta t} \int_{1+(j-\frac{1}{2})h}^{1+(j+\frac{1}{2})h} A(x) \left| (R_i(\rho_{10}^h(x, t), \rho_{20}^h(x, t)) \right.$$

$$\left. - R_i(\rho_{10}^h(x, n\Delta t - 0), \rho_{20}^h(x, n\Delta t - 0)))\bar\psi(x, t) \right| dxdt$$

$$+ \sum_{j,n} \int_{(n-1)\Delta t}^{n\Delta t} \int_{1+(j-\frac{1}{2})h}^{1+(j+\frac{1}{2})h} \left| R_i(\rho_{10}^h(x, n\Delta t - 0), \rho_{20}^h(x, n\Delta t - 0)) \right.$$

$$\left. \times (\bar\psi(x, t) - \bar\psi_j^n) \right| dxdt$$

$$\le \|\psi\|_{C_0^1} \sum_{i=1,2} \sum_{j,n} \int_{(n-1)\Delta t}^{n\Delta t} \int_{1+(j-\frac{1}{2})h}^{1+(j+\frac{1}{2})h} \left| \rho_{i0}^h(x, t) - \rho_{i0}^h(x, n\Delta t - 0) \right| dxdt$$

$$+ \|\psi\|_{C_0^1}(O(h) + O(h^\beta))$$

$$\le \|\psi\|_{C_0^1}(O(h) + O(h^\beta)).$$

By Lemma 3.6,

$$
\begin{aligned}
&|I_{12}| \\
&\leq C\|\bar{\psi}\|_{C_0^1}\sqrt{h} \\
&\quad \times \left(\sum_{j,n} \int_{1+(j-\frac{1}{2})h}^{1+(j+\frac{1}{2})h} (|\rho_0^h(x, n\Delta t - 0) - \rho_j^n|^2 + |\rho_j^n - \rho_0^h(x, n\Delta t + 0)|^2)dx \right)^{\frac{1}{2}} \\
&\leq O(\sqrt{h})\|\bar{\psi}\|_{C_0^1}.
\end{aligned}
$$

Therefore

$$
\begin{aligned}
&\int\int_{\Pi_T} (\rho^h \psi_t + m^h \psi_x + a(x)m^h\psi)dxdt + \int_1^2 \rho_0^h(x)\psi(x, 0)dx \\
&= \|\bar{\psi}\|_{C_0^1}(O(h) + O(h^\beta) + O(\sqrt{h})) + \|\psi\|_{H^1}O(h^\beta) \to 0, \quad h \to 0.
\end{aligned}
$$

Taking the limit $h \to 0$ on both sides and using the dominated convergence theorem, we have

$$
\int\int_{\Pi_T} (\rho\psi_t + m\psi_x + a(x)m\psi)dxdt + \int_1^2 \rho_0(x)\psi(x, 0)dx = 0.
$$

Following the similar estimates in [8], we have

$$
\int\int_{\Pi_T} \left(m\psi_t + \left(\frac{m^2}{\rho} + p(\rho) \right)\psi_x + \left(a(x)\frac{m^2}{\rho} + G_2(u_1, u_2, x, t) \right)\psi \right)dxdt
$$

$$
+ \int_1^2 m_0^h(x)\psi(x, 0)dx = 0,
$$

and, for any convex weak entropy pair (η, q), the limit function $u = (\rho, m)$ satisfies

$$
\eta(u)_t + q(u)_x - (a(x)g(u) + G(u, x, t))\nabla\eta(u) \leq C,
$$

in the sense of distributions. Using the standard procedure (cf. [21]), we conclude that the limit function $u(x, t)$ satisfies the entropy condition (3.13) along any shock wave. The uniform boundedness of $u^h(x, t)$ implies the boundedness of the weak solution $u(x, t)$.

The initial-boundary values can be recovered by the detailed estimates similar to [8] on the traces, which are properly defined along the boundaries. □

3.4　Nozzle Solutions

Now we consider the following equations for the nozzle flow:

$$
\begin{cases}
(A\rho_i)_t + (Am_i)_x = AG_1, \\
(Am_i)_t + (A\frac{m_i^2}{\rho_i})_x + Ap(\rho_i)_x = AG_2, \quad i = 1, 2,
\end{cases}
\tag{3.14}
$$

$1 < x < 2$, $t > 0$,   with initial-boundary conditions:

$$\begin{cases} (\rho_i, m_i)|_{t=0} = (\rho_{i0}(x), m_{i0}(x)), \\ m_i|_{x=1} = m_i|_{x=2} = 0, \end{cases} \tag{3.15}$$

where $A(x) \in C^2$ represents the cross-sectional area of the nozzle at x, and G_1 and G_2 are the same as in (3.2).

The system (3.14) is equivalent to

$$\begin{cases} \partial_t \rho_i + \partial_x m_i = a(x)m_i + R_i(\rho_1, \rho_2), \\ \partial_t m_i + \partial_x \left(\frac{m_i^2}{\rho_i} + p(\rho_i) \right) = a(x)\frac{m_i^2}{\rho_i} + G_2(\rho_1, m_1, \rho_2, m_2, x, t), \quad i = 1, 2, \end{cases} \tag{3.16}$$

where $a(x) = -\frac{A'(x)}{A(x)}$.

As earlier in Section 3, we construct the approximate solutions $(\rho_i^h, m_i^h)(x, t)$ of (3.16) and then prove that the approximate solutions satisfy the compensated compactness framework (Lemma 3.8) as for (3.1). Then we conclude that there is a subsequence of the approximate solutions strongly convergent to the L^∞ function $(\rho_i(x, t), m_i(x, t))$ almost everywhere. We obtain:

Theorem 3.10 *Assume that the initial data (ρ_0, u_0) are bounded in L^∞. Then there exists a bounded weak entropy solution $(\rho_i(x, t), m_i(x, t))$ of (3.14–3.15) in the sense of Definition 3.7.*

4   The Simulation of the Gunn Diode

The numerical scheme we use in the simulations is the third order ENO (Essentially Non-Oscillatory) schemes based on point values and Runge-Kutta time discretizations [28]. The description of this scheme applied to the hydrodynamic models can be found in [18], hence will not be repeated here.

The two valley GaAs hydrodynamic model we use for this purpose, in one space dimension, has the following form, where j is to be selected distinct from i:

$$\begin{aligned} \partial_t \rho_i + \partial_x(\rho_i v_i) &= -\frac{\rho_i}{\tau_{nij}} + \frac{m_i^*}{m_j^*}\frac{\rho_j}{\tau_{nji}}, \\ \partial_t(\rho_i v_i) + \partial_x(\rho_i v_i^2 + p_i) &= -\frac{e}{m_i^*}\rho_i F - \frac{\rho_i v_i}{\tau_{pi}}, \\ \partial_t E_i + \partial_x[v_i(E_i + p_i)] &= -\frac{e}{m_i^*}\rho_i v_i F - \frac{E_i - \frac{3}{2}\frac{k_b}{m_i^*}\rho_i \mathcal{T}_0}{\tau_{wii}} \\ &\quad - \frac{E_i}{\tau_{wij}} + \frac{E_j}{\tau_{wji}} + \partial_x(\kappa_i \partial_x \mathcal{T}_i), \end{aligned} \tag{4.1}$$

for $i, j = 1, 2$ and $i \neq j$. Here, $\rho_i = m_i^* n_i$ are the particle densities, with n_i denoting the concentration, v_i are the particle velocities, E_i are the total energies, $p_i = (\gamma - 1)(E_i - \frac{1}{2}\rho_i v_i^2)$ are the pressures, with constant $\gamma = \frac{5}{3}$, $\mathcal{T}_i = \frac{m_i^* p_i}{k_b \rho_i}$ are

the temperatures. The equation (4.1) is coupled with the potential equation,

$$\epsilon \partial_x^2 \phi = e(n_1 + n_2 - n_d) \tag{4.2}$$

through the electric field term $F = -\partial_x \phi$. The relaxation terms are defined by

$$\frac{1}{\tau_{n12}} = \frac{1}{\tau_{p12}} = \begin{cases} 0, & if & E_1 \leq \alpha n_1(1-\beta), \\ smooth, & if & \alpha n_1(1-\beta) < E_1 < \alpha n_1(1+\beta), \\ 30, & if & E_1 \geq \alpha n_1(1+\beta), \end{cases} \tag{4.3}$$

where α is a threshold controlling the amount of coupling between the valleys, and turns out to be crucial for the simulation. This will be discussed in more detail later. β is chosen to smooth the relaxation expressions. In our computation $\beta = 0.15$ is used. The smooth connection between the two constant values 0 and 30 in (4.3) is achieved by a polynomial which makes the expression globally C^3. Other relaxation terms are defined by

$$\frac{1}{\tau_{n21}} = \frac{1}{\tau_{p21}} = 2, \qquad \frac{1}{\tau_{p11}} = 7, \qquad \frac{1}{\tau_{p22}} = 20, \tag{4.4}$$

$$\frac{1}{\tau_{p1}} = \frac{1}{\tau_{p11}} + \frac{1}{\tau_{p12}}, \qquad \frac{1}{\tau_{p2}} = \frac{1}{\tau_{p22}} + \frac{1}{\tau_{p21}}, \tag{4.5}$$

$$\tau_{w11} = 2\tau_{p11}, \qquad \tau_{w22} = 2\tau_{p22}, \qquad \tau_{w12} = 2\tau_{n12}, \qquad \tau_{w21} = 2\tau_{n21}. \tag{4.6}$$

The heat conduction term κ_i is defined by

$$\kappa_i = \frac{3\mu_{0i}k_b^2 \mathcal{T}_0}{2e} n_i \tag{4.7}$$

where $\mu_{0i} = \frac{e\tau_{pi}}{m_i^*}$. The values of other parameters used in the simulations (in our units) are: $m_1^* = 0.065 m_e^*$, $m_2^* = 0.222 m_e^*$ with $m_e^* = 0.9109$; $e = 0.1602$; $k_b = 0.138046 \times 10^{-4}$; $\epsilon = 12.9 \times 8.85418$; $\mathcal{T}_0 = 300$. The doping n_d is defined by

$$n_d(x) = \begin{cases} 10^5, & 0 \leq x \leq 0.125 - \beta_1 \\ 10^4, & 0.125 + \beta_1 \leq x \leq 0.15 - \beta_1 \\ 5 \times 10^3, & 0.15 + \beta_1 \leq x \leq 0.1875 - \beta_1 \\ 10^4, & 0.1875 + \beta_1 \leq x \leq 1.875 - \beta_1 \\ 10^5, & 1.875 + \beta_1 \leq x \leq 2 \\ smooth, & otherwise \end{cases} \tag{4.8}$$

where again "smooth" means a connection by a polynomial to make the doping globally C^3 and the smoothing length is chosen as $\beta_1 = 0.005$. We show the doping, in a logarithm scale, in Fig. 2.
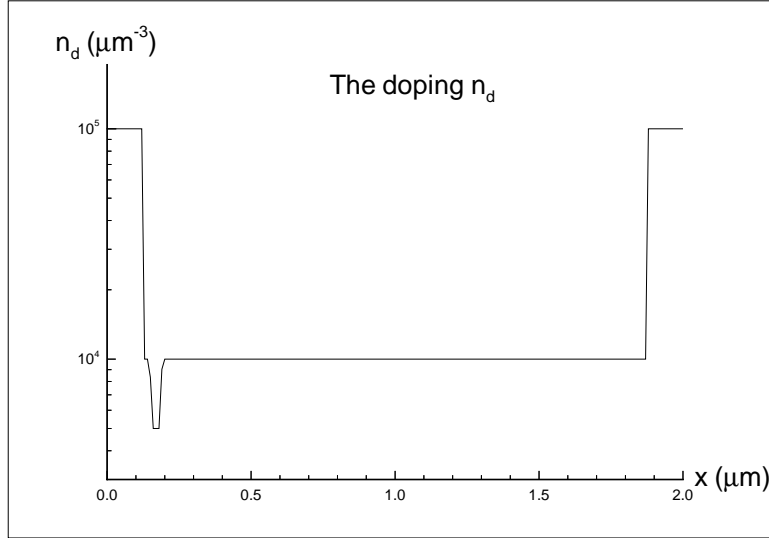
Fig. 2: One dimensional two valley hydrodynamic model. The doping n_d (in logarithm scale).

Boundary conditions are chosen as follows: for the concentration n_i, we fix them at both ends with $n_1 = n_d$ and $n_2 \approx 0$. Technically, n_2 cannot be zero in the code, hence a small number $n_2 = 10^{-5}$ is used instead. The temperatures $\mathcal{T}_i$ are also fixed at both ends, with $\mathcal{T}_i = \mathcal{T}_0$. The velocity v_i satisfies a Neumann boundary condition (numerically it corresponds to zeroth order extrapolation). The potential ϕ is fixed at both ends with a voltage difference determined by *vbias* (the voltage bias): we take $\phi = 0$ at the left end $x = 0$, and $\phi = vbias = 2\text{V}$ at $x = 2$ for the stand alone device, and $\phi = V_d(t)$ at $x = 2$, if the system is coupled with the Gunn oscillator (1.1).

For the stand alone device, we would like to reach a steady state solution of the system (4.1)-(4.2). We thus start from the following initial condition: $n_1(x, 0) = n_d(x)$, $n_2(x, 0) = 10^{-5}$, $v_i(x, 0) = 0$, $\mathcal{T}_i(x, 0) = \mathcal{T}_0$, and compute the time evolution of the system until it reaches a steady state. In practice, in order to achieve a steady state more rapidly, a continuation in *vbias* is used, by starting from $vbias = 0.0\text{V}$, and each time increasing it in increments of $0.05V$, by using the previous steady state as the initial condition for the higher value of *vbias*, until a steady state for the choice $vbias = 2\text{V}$ is reached. This steady state solution is used as the initial condition for the Gunn oscillator, when the system (4.1)-(4.2) is coupled with the ODE (1.1).

It turns out that the coupling of the two valleys in the model, through an energy transfer, is crucially dependent upon the coupling threshold α in (4.3). The higher the threshold value, the lower the coupling effect becomes, as expected. Fig. 3 shows the concentration n_i of the two valleys in steady states, for different values of α.
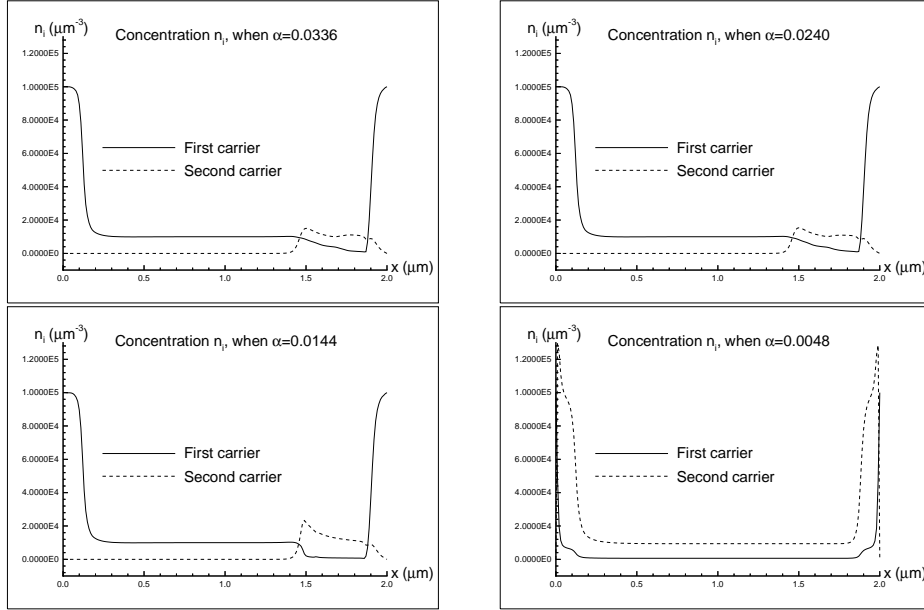
Fig. 3: One dimensional two valley hydrodynamic model. Concentrations n_i for both valleys at various coupling thresholds: $\alpha = 0.0336$, 0.0240, 0.0144 and 0.0048.

To conform with physics, and the Monto-Carlo simulation results in [22], we choose $\alpha = 0.0144$ for our simulation with the Gunn oscillator. The ODE (1.1) is coupled to the two valley hydrodynamic model (4.1)-(4.2), through the application of $V_D(t)$ as the boundary condition for the potential equation (4.2) at the right end $x = 2$. Other parameters in (1.1), expressed in values consistent with our units, are $V_B = vbias = 2$, $L = 3.5 \times 10^{-6}$, $C = \frac{\epsilon A}{W} + 0.82 \times 10^6$ with $A = 10^3$ and the device length $W = 2$, $R = 25 \times 10^{-6}$, and $I_d(t) = \frac{1}{W} \int_0^W I_e(x,t)dx$, with $I_e(x,t) = -eA(n_1(x,t)v_1(x,t) + n_2(x,t)v_2(x,t))$. The initial condition for the ODE (1.1) is chosen as $I(0) = 0$ and $V_D(0) = 2$. When the oscillator is coupled to the hydrodynamic system, after an initial transition, a time periodic solution results. In Fig. 4, we show the time history of the applied voltage $V_D(t)$ (left) and the current flowing through the battery $I(t)$ (right) after the initial transition. These are the two variables in the ODE (1.1), and clearly they show sustained oscillations of a slow frequency layered over a fast frequency.
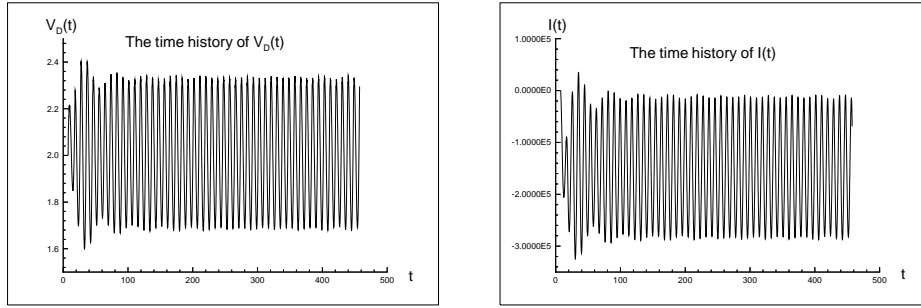
Fig. 4: One dimensional two valley hydrodynamic model, coupled with the Gunn oscillator. Left: the voltage at the device terminal $V_D(t)$; Right: the current flowing through the battery $I(t)$.

We would like to point out that, since the simulation here involves a time dependent system with strong hyperbolic components, which must be simulated for a very long time, upwinding and high order accuracy in space and time are important, justifying the usage of ENO schemes. Next, in Fig. 5, we show the concentration n_i, the velocity v_i, and the temperature $\mathcal{T}_i$ of both carriers, at 4 equally spaced "snaps" over one period of the oscillation. We can see the movement, or "precession", of the structure clearly in such a period.
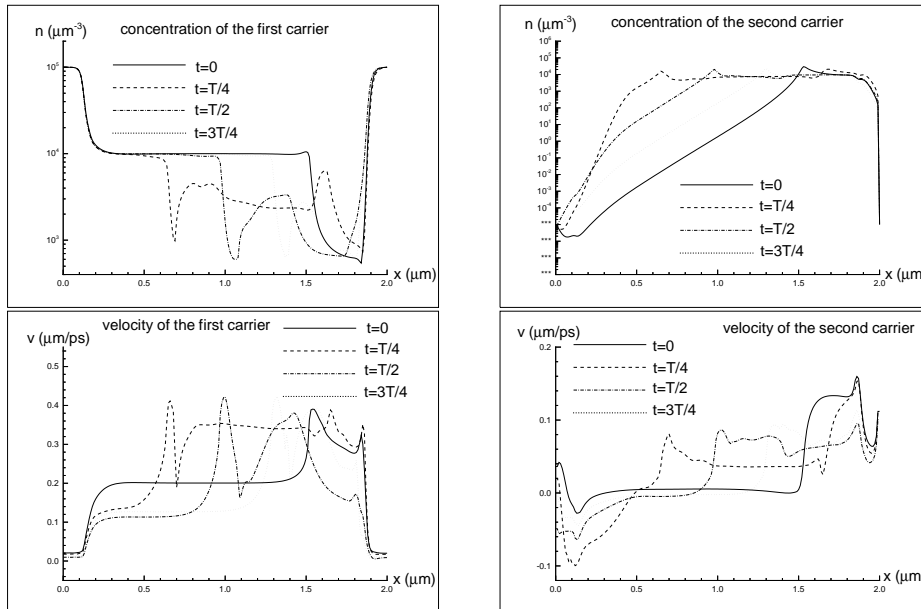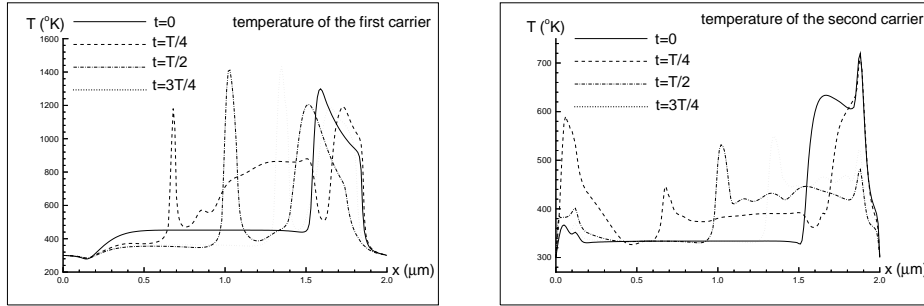
Fig. 5: One dimensional two valley hydrodynamic model, coupled with the Gunn oscillator. Four equally spaced "snaps" over one period of the oscillation. Top: concentration n_i; Middle: velocity v_i; Bottom: temperature $\mathcal{T}_i$. Left: the first valley $i = 1$; Right: the second valley $i = 2$.

5   The Simulation of the MESFET: Symmetry and Symmetry-Breaking

The motivation of this section is as follows: if some symmetry exists for the two dimensional (2D) MESFET, which is relatively costly to simulate, we can use this information to reduce our model to 1D, at least for some components, thereby reducing the cost of simulation. For this purpose, we first look at the 2D simulation results at various values of *vbias*. The boundary condition at the gate is always taken as *vbiasgate* $= -0.4vbias$. The simulation is the same as those in [18], using a third order ENO scheme and 192×64 grid points. The result is shown in Figs. 6-9.
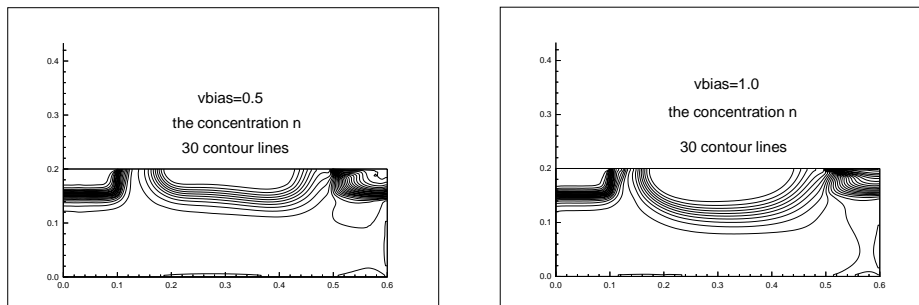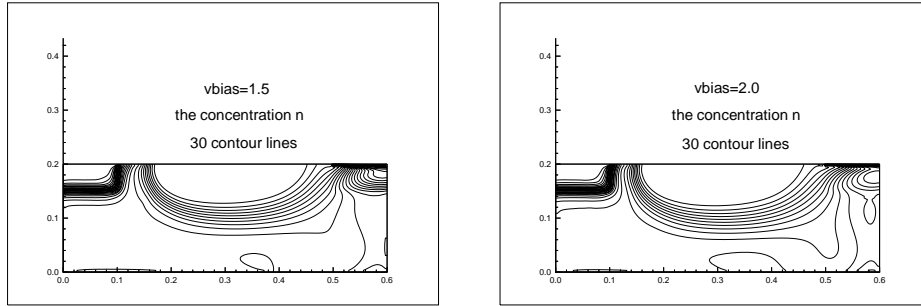
Fig. 6: Two dimensional MESFET. Simulation result at $vbias = 0.5$V, 1.0V, 1.5V and 2.0V. The concentration n.
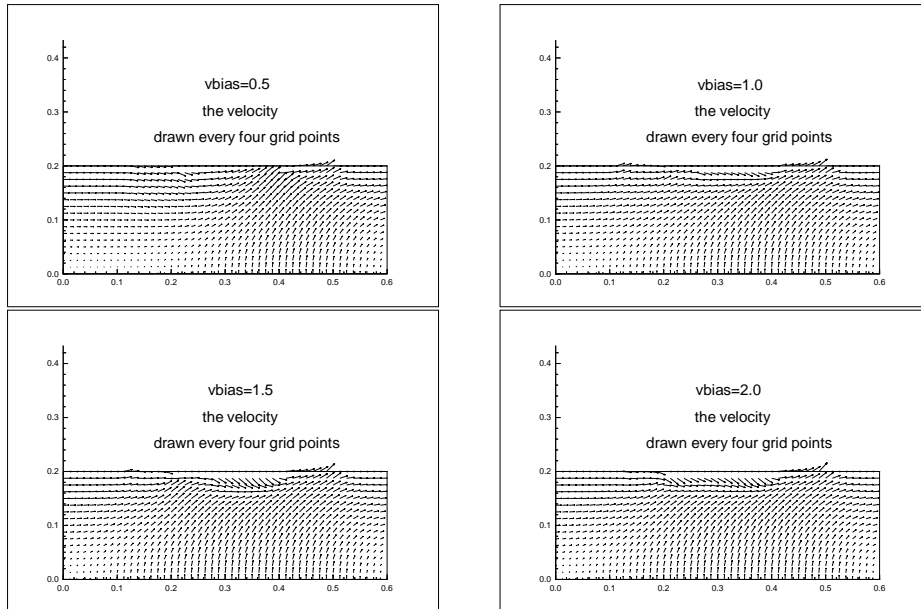
Fig. 7: Two dimensional MESFET. Simulation result at $vbias = 0.5$V, 1.0V, 1.5V and 2.0V. The velocity vector $\vec{v}$.
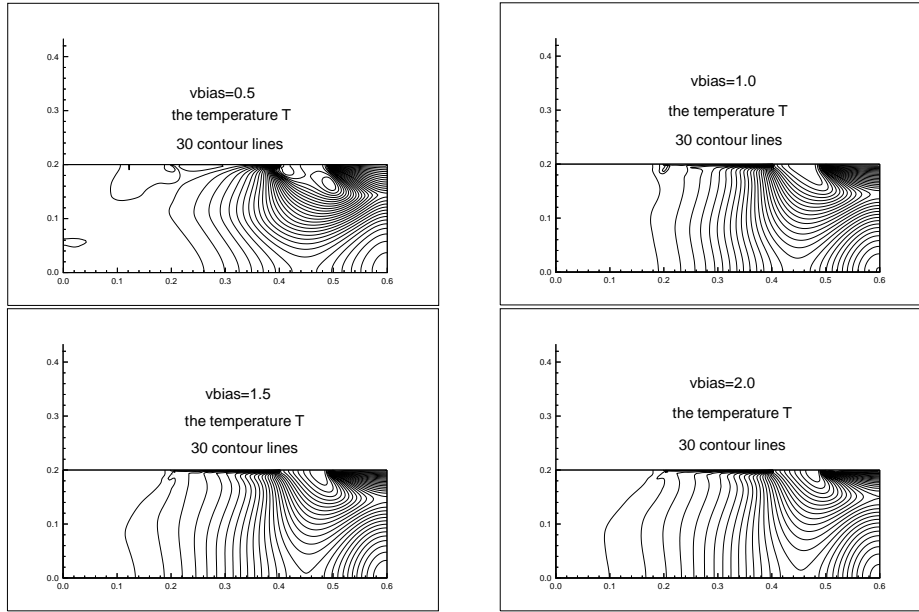
Fig. 8: Two dimensional MESFET. Simulation result at *vbias* = 0.5V, 1.0V, 1.5V and 2.0V. The temperature T.
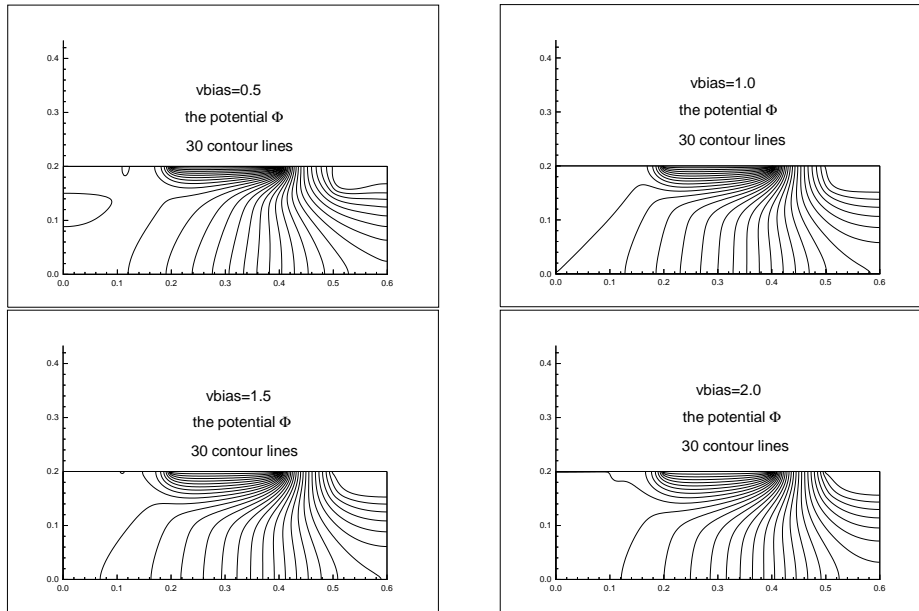
Fig. 9: Two dimensional MESFET. Simulation result at *vbias* = 0.5V, 1.0V, 1.5V and 2.0V. The potential ϕ.

We can see from these figures that, for larger values of *vbias*, only concentration is approximately spherically symmetric around the top middle point $(x, y) = (0.3, 0.2)$.

Next, we show the result of trying to use the 1D model with a spherical symmetry assumption, to approximate the 2D MESFET described in Section 1.2. We take our 1D domain from $r = 0.025$ to $r = 0.1$, measured from the top middle point at $(x, y) = (0.3, 0.2)$ downward. The boundary conditions for the concentration n, the temperature $\mathcal{T}$ and the potential ϕ are prescribed, using the values of the 2D simulations; the boundary condition for the velocity is floating (Neumann). In Fig. 10, we show the comparison, for the concentration n, of the 2D MESFET result with the 1D model assuming spherical symmetry, at $vbias = 0.5\text{V}, 1.0\text{V}, 1.5\text{V}$ and 2.0V. We can clearly see a qualitatively correct agreement. This is very promising since it means that other quantities (such as $\mathcal{T}$ and ϕ) which are not spherically symmetric have minimal effect on the concentration through the nonlinear coupling of the equations.
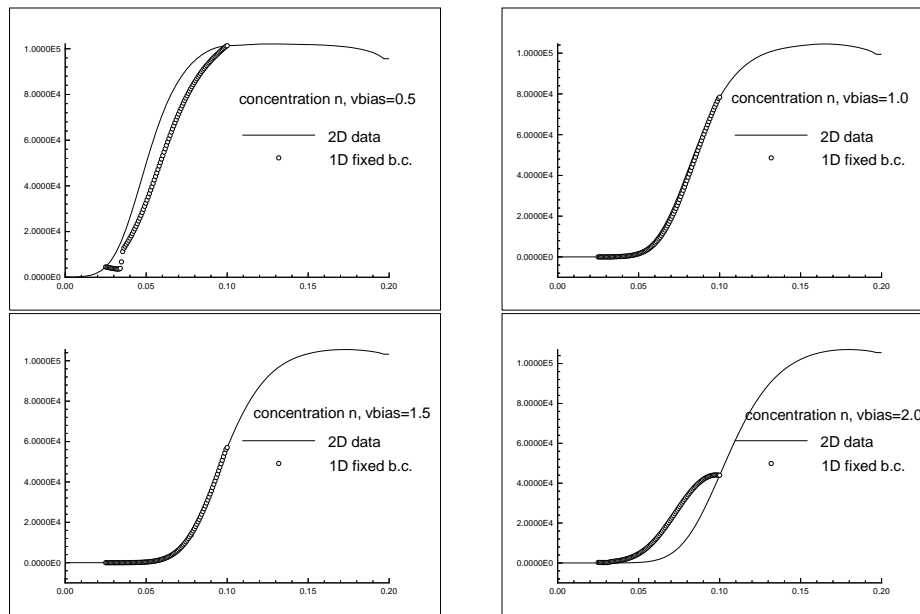
Fig. 10: The 1D model with spherical symmetry assumption, in comparison with the 2D MESFET results, at $vbias = 0.5\text{V}, 1.0\text{V}, 1.5\text{V}$ and 2.0V. The concentration n.

Next, we show the same comparison for the temperature $\mathcal{T}$ in Fig. 11. We can see that now the 1D model is at much greater variance with the 2D results, manifesting the fact that $\mathcal{T}$ is not spherically symmetric. Pictures for v and ϕ show similar discrepancies. If n is the only quantity of interest, then the 1D model can be used, saving substantial computing time in the simulation.

Otherwise, a better model (perhaps a hybrid one with the non-symmetric components computed by the 2D model and symmetric quantities computed by the 1D model) might be useful.

Fig. 11: The 1D model with spherical symmetry assumption, in comparison with the 2D MESFET results, at $vbias = 0.5$V, 1.0V, 1.5V and 2.0V. The temperature $\mathcal{T}$.

Bibliography

1. Bløtekjær, K. (1970). Transport equations for electrons in two–valley semiconductors. *IEEE Trans. Electron Devices*, **17**, 38–47.

2. Chen, G.-Q. (1988). Convergence of (the) Lax-Friedrichs scheme for isentropic gas dynamics, III. *Acta Math. Scientia*, **8**, 243–276. (in Chinese): **6**, 75–120, 1986.

3. Chen, G.-Q. (1990). The compensated compactness method and the system of isentropic gas dynamics. *MSRI Preprint 00527-91*. Berkeley.

4. Chen, G.-Q. (1997). Remarks on spherically symmetric solutions to the compressible Euler equations. *Proc. Royal Soc. Edinburgh*, to appear.

5. Chen, G.-Q. and Glimm, J. (1996). Global solutions to the compressible Euler equations with geometrical structure. *Commun. Math. Phys.* **180**: 153-193.

6. Chen, G.-Q. and Glimm, J. (1996). Global solutions to the cylindrically symmetric rotating motion of isentropic gases. *Z. Angew. Math. Phys.* **47**: 353-372.

7. Chen, G.-Q., Jerome, J. W. and Zhang, B. (1997). Particle hydrodynamic moment models in biology and microelectronics: singular relaxation limits. *To appear in Proceedings of the 2nd World Congress of Nonlinear Analysts, Athens, Greece.*

8. Chen, G.-Q. and Wang, D. (1996). Convergence of shock capturing schemes for the compressible Euler-Poisson equations. *Commun. Math. Phys.* **179**: 333-364.

9. Curow, M. and Hintz, A. (1987). Numerical simulation of nonstationary electron transport in Gunn devices in a harmonic mode oscillator circuit. *IEEE Trans. Electr. Dev.*, ED-**34**, 1983–1994.

10. Dafermos, C. (1972). Polygonal approximations of solutions of the initial-value problem for a conservation law. *J. Math. Anal. Appl.*, **38**, 33–41.

11. Ding, X., Chen, G.-Q. and Luo, P. (1987/88). Convergence of the Lax-Friedrichs scheme for isentropic gas dynamics (I)-(II). *Acta Math. Scientia*, **7**, 467–480; **8**, 61–94. (in Chinese): **5**, 415–432, 433–472, 1985.

12. DiPerna, R. (1983). Convergence of the viscosity method for isentropic gas dynamics. *Commun. Math. Phys.*, **91**, 1–30.

13. Embid, P., Goodman, J. and Majda, A. (1984). Multiple steady states for 1-D transonic flow. *SIAM J. Sci. Stat. Comp.*, **5**, 21–41.

14. Fang, W. and Ito, K. Weak solutions to a one-dimensional hydrodynamic model of two carrier types for semiconductors. *Preprint.*

15. Glaz, H. and Liu, T.-P. (1984). The asymptotic analysis of wave interactions and numerical calculation of transonic nozzle flow. *Adv. Appl. Math.*, **5**, 111–146.

16. Glimm, J., Marshall, G. and Plohr, B. (1984). A generalized Riemann problem for quasi-one-dimensional gas flow. *Adv. Appl. Math.*, **5**, 1–30.

17. Jerome, J. W. (1996). *Analysis of Charge Transport: A Mathematical Study of Semiconductor Devices*, Springer-Verlag, Heidelberg.

18. Jerome, J. W. and Shu, C.-W. (1994). Energy models for one-carrier transport in semiconductor devices. In *IMA Volumes in Mathematics and Its Applications*, v.59 (eds. Coughran, W., Cole, J., Lloyd, P. and White, J.) pp. 185–207. Springer.

19. Jerome, J. W. and Shu, C.-W. (1995). Transport effects & characteristic modes in the modeling & simulation of submicron devices. IEEE Trans. on Computer–Aided Design, **14**, 917–923.

20. Jerome, J. W. and Shu, C.-W. (1995). The response of the hydrodynamic model to heat conduction, mobility, and relaxation expressions. VLSI Design, **3**, 131–143.

21. Lax, P.D. (1973) *Hyperbolic Systems of Conservation Laws and the Mathematical Theory of Shock Waves*. C.B.M.S. 11. SIAM.

22. Lee, C.H. and Ravaioli, U. (1991). Transient Monte-Carlo simulation of heterojunction microwave oscillators. In *Computational Electronics* (eds. Hess, K., Leburton, J.P. and Ravaioli, U.) pp. 169–172. Kluwer Academic Publishers.

23. Liu, T.-P. (1979). Quasilinear hyperbolic systems. *Comm. Math. Phys.*, **68**, 141–172.

24. Liu, T.-P. (1987). Nonlinear resonance for quasilinear hyperbolic equations. *J. Math. Phys.*, **28**, 2593–2602.

25. Makino, T. and Takeno, S. (1994). Initial boundary value problem for the spherically symmetric motion of isentropic gas. *Japan J. Indust. Appl. Math.*, **11**, 171–183.

26. Natalini, R. (1996). The bipolar hydrodynamic model for semiconductors and the drift-diffusion equations. *J. Math. Anal. Appl.*, **198**, 262–281.

27. Selberherr, S. (1984). *Analysis & Simulation of Semiconductor Devices*, Springer-Verlag, Wien-New York.

28. SHU C.-W. and OSHER, S.J. (1989). Efficient implementation of essentially non-oscillatory shock capturing schemes, II. *J. Comp. Phys.*, **83**, 32–78.

29. Tartar, L. (1979). *Compensated compactness and applications to partial differential equations*. Research Notes in Mathematics, Nonlinear Analysis and Mechanics, v.4. (ed. Knops, R.J.). Pitman Press.